Journal of the Indian Society of Remote Sensing (June 2020) 48(6):877–908
https://doi.org/10.1007/s12524-020-01122-7

RESEARCH ARTICLE

Evaluation of Classification Techniques for Land Use Change Mapping of Indian Cities

Vidhee Avashia[1] · Shrutika Parihar[2] · Amit Garg[1]

Received: 4 October 2019 / Accepted: 30 May 2020 / Published online: 20 June 2020

Abstract
This study looks into the development of multi-level classification approach for land use change mapping in Indian cities using Landsat imageries. In this study, we mapped 47 Indian cities at different time frames 1990, 2000, 2010, and 2017. We started with traditional classification methods, but results provided unsatisfactory accuracy levels. Thus, we employed multiple classification techniques to achieve results with higher accuracy. The paper captures the evaluation of different classification techniques—hybrid, unsupervised, decision tree classification (DTC), and object-based image analysis (OBIA). The results suggest improvement in accuracy levels by using multi-level classification for different cities at different stages of the classification process. The most prominent is the hybrid classification technique; 14 cities out of 47 reached to accuracy above 72% through hybrid classification. For problematic classes, we used DTC, OBIA, and unsupervised classification techniques after masking the datasets. DTC was used in cities with a greater number of problems in datasets. For example, in the case of Kochi City, the accuracy at the initial level was reported 51% through unsupervised classification which improved to 77% (supervised classification), and finally, it reached 90% by DTC technique. The overall accuracy achieved through the multi-level classification approach described in this paper for the 47 Indian cities ranges from 81 to 93%.

Keywords Multi-level classification · Cities · Accuracy · Hybrid · Unsupervised · DTC · OBIA · India

Introduction

The term "land use'' usually relates to the human activity associated with a specific area of land, and (Sharma et al. 1984) "land cover is the observed (bio-) physical cover on the earth's surface" (Di Gregorio and Jansen 1998). Land use and land cover (LU/LC) represent the integration of various elements of resources like water, atmosphere, climate, and land. Thus, changes in LU/LC over time significantly affect these resource systems at a global as well as local scale (Meyer and Turner 1992). LU/LC is one of the most important aspects to build understanding and linkages between man and environment. It is a dynamic phenomenon that requires continuous monitoring and mapping. Satellite imagery is a powerful tool for tracking down these changes. Satellite imageries are used to collect information for the strategic planning of land-based resources. Landsat has been successfully running as the oldest satellite program in the world for the past 45 years. A synoptic temporal coverage of LU/LC is the major advantage of the Landsat satellite. Multispectral and multitemporal continuous scanning of earth surface by Landsat satellite facilitates applications in forestry, urban sprawl, agriculture, vegetation (McCallum et al. 2006). Hence, Landsat imageries are extensively used in LU/LC studies for image classification processes and mapping.

Landsat data acquired for different periods encompass consistent geometry throughout the region. When the Landsat database is collected and the images are mosaiced to cover the study area or region, the most important assumptions here are that images have consistent geometry and uniform spatial resolution. These assumptions have been considered to be consistent for Landsat satellite

✉ Amit Garg
amitgarg@iima.ac.in

[1] Public Systems Group, Indian Institute of Management Ahmedabad, Ahmedabad, Gujarat, India

[2] Global Centre for Environment and Energy, Ahmedabad University, Ahmedabad, Gujarat, India

despite sensor upgradation starting from multi-spectral scanner (MSS), thematic mapper (TM), enhanced thematic mapper plus (ETM+), and operational land imager (OLI) for achieving increased image overall accuracy over time (Morfitt et al. 2017; Rozenstein and Karnieli 2011; Storey and Choate 2000; Bryant et al. 1995).

The geodetic accuracy of the Landsat dataset has also improved over the years from the 1970s, 1990s, and 2000s, indicating high research potential. Landsat data have 30 m resolution and positional accuracy of less than 50 m root mean square (RMS) error (Tucker et al. 2004). Ma et al. (2017) compare the mean classification accuracy of twelve different types of sensors to find that the highest is reported by UAV and Spot-5 sensors at 86%, whereas Landsat accounts 83% mean overall accuracy of the sensor, indicating that Landsat data are equally conscientious (Ma et al. 2017).

The newest generation satellites do not allow historical evaluations, such as long-term time series analysis or decadal change study (Tarantino et al. 2015; Fichera et al. 2012). Landsat is the only satellite that provides datasets from 1972 to 2018. Landsat dataset also offers an extensive range of scientific methods and applications worldwide (Phiri and Morgenroth 2017; Song et al. 2014; Wulder et al. 2012). Landsat's free data access policy facilitates the creation of a large quantum of comparable data across time and across cities. Thus, for the study on tracing the decadal changes in LU/LC across 47 cities in India, we opted for the Landsat dataset.

The study described here traces the spatiotemporal changes of 47 cities of India for years 1990, 2000, 2010 and 2017, showing urban growth pattern and evaluating the land use change matrix, e.g., tracing changes in green and blue spaces in and around the cities. The purpose of this massive exercise is to inform the urbanization growth process and related issues to the national agencies and local governments of India. The objective of this paper is to acquire a better insight into achieving higher classification accuracies for all images processed for different time frames, across all land cover classes by using multiple classification techniques. The construction process of the final database for 47 cities consisted of dealing with different issues that have been reasonably resolved by opting for different classification techniques to enhance the classification accuracy at each stage of processing.

Review of Different Techniques and Multi-level Classification

Land use classification is a complex process. Various factors such as opting for suitable classification techniques, selection of appropriate training samples, image processing, mosaicing, feature extraction, preprocessing, and post-processing of images have a role to play in the outcome. Designing the methodology should thus be informative, exhaustive, and separable at each stage. Another foremost imperative element of the image classification technique is to have analyst's skills which help to define the probable classification approach such as the classification scale to achieve high accuracy.

There are several studies concerned with specific image classification techniques. However, there is a lack of studies looking into guidelines for choosing suitable classification techniques/approaches (Lu and Weng 2007). In recent years, new classification algorithms and techniques such as the combination of multiple classification techniques have emerged. Each classification technique possesses its strengths and limitations (Mather and Tso 2009). Combination of one or more classification techniques not only improves the classification results but also brings better accuracy level as compared to single classification technique (Warrender and Augusteijn 1999; Congalton and Green 2019; Masocha and Skidmore 2011; Nicholas 2012; Zhao et al. 2016). Many researchers have explored different classification techniques like regression methods, majority voting, production rule, the sum rule, and threshold values to integrate multiple classification techniques that enhance results (Steele 2000; Liu et al. 2004; Schweitzer et al. 2005; Mohammady et al. 2015).

In multisource (TM, ETM+, and OLI) data, the combination of multiple classification techniques gives more precise information on parameters like spectral signatures, texture and context information, the accuracy of classification techniques. Traditionally most classifiers have been grounded to a significant degree in statistical decision theory and grouped into parametric and nonparametric classifiers. A parametric classifier is largely governed by how strong the data match with the predefined models and are dependent on the accuracy assessment of these model parameters. Most of the popular and useful parametric classifiers are based on maximum likelihood algorithms. However, there are disadvantages of using them in land use classification due to uncertainties around the distribution of land use classes which cannot be described based on the distribution of data (Caetano 2007). Nonparametric classifiers most popularly used in LU/LC are the artificial neural network, decision tree classification techniques, and use of knowledge-based classification techniques. These methods are significantly more appropriate to handle ambiguous data processes and hence may prove to be advantageous in land use classification (Liu et al. 2004; Choodarathnakara et al. 2012; Ma et al. 2017). Selection of suitable classifier depends on many factors such as the aim of classification type, use of ancillary data, classification system, software, algorithm performance, computational

Table 1 Land use classification techniques and accuracy

Classification technique	Types of classifiers	Images (Landsat) used	LU/LC classes	Accuracy level (%)	Sources
Supervised	Maximum likelihood, nearest neighbor and support vector machine	TM, OLI	Urban	73–82	Phiri and Morgenroth (2017)
		TM, OLI	Forest	52–90	Phiri and Morgenroth (2017)
		OLI	Agriculture	80–87	Rwanga and Ndambuki (2017) and Tilahun and Teferie (2015)
		TM, ETM+	Water	83–88	Manandhar et al. (2009)
		OLI	Mangrove	82–89	Islam et al. (2018) and Rahman et al. (2013)
Unsupervised	ISODATA	TM	Urban	78–94	S1
		TM	Forest	58–81	Alrababah and Alhamad (2006) and Sader et al. (1995)
		TM	Agriculture	55–74	Rozenstein and Karnieli (2011) and Sharma et al. (2013)
		MSS, ETM+	Water	30–50	Adejoke and Badaru (2014) and Sharma et al. (2013)
		OLI	Mangrove	70–86	Islam et al. (2018)
Object based	Support vector machine, decision tree classifier, nearest neighbor	ETM+, TM, MSS, OLI	Urban	73–98	Phiri and Morgenroth (2017)
	Decision tree classifier	TM	Forest	77–95	Phiri and Morgenroth (2017)
	Support vector machine, decision tree classifier	ETM+, TM	Water	71–98	Chang et al. (2014) and Hecher et al. (2012)
	Decision tree classifier	TM	Agriculture	76–90	Phiri and Morgenroth (2017)
	Support vector machine, decision tree classifier, nearest neighbor	MSS, TM, ETM+, OLI	Mangrove	77–84	Son et al. (2015)

resources, accuracy, purpose, and duration of the research (DeFries and Chan 2000; Zhang et al. 2002; Keuchel et al. 2003; Pal and Mather 2003; Atkinson and Aplin 2004). Table 1 describes the various classification techniques and their possible accuracy levels across various LU/LC classes.

Data Preparation

The research study uses Landsat Thematic Mapper as a major data source for analysis of LU/LC of 47 cities of India spreading across different climatic zones and size classes as listed in Table 2. The study was carried out on multi-temporal optical remote sensing data for the periods of 1990, 2000, 2010, and 2017. These satellite images were classified by using multi-level classification processes that employ digital and visual image interpretation techniques. The images were masked at the city level as per their latest municipal boundaries obtained from city development plan and master plan documents of the city governments. In our research, we have opted for the land use II level of classification as per the National Natural Resources Management System (NNRMS) guidelines set up by the Government of India.

Methodology for Data Processing

The purpose of this paper is to explore different classification techniques that facilitate in obtaining accurate results for LU/LC classification. The research methodology is divided into various stages: data collection, pre-processing, a combinative approach of multiple classification techniques and post-processing (Fig. 1).

The study uses a combinative approach of two or more classification techniques to find the best results.

Landsat images downloaded from the U.S. Geological Survey (USGS) Earth explorer were stacked in ENVI 5.4 software. City boundaries were extracted from the secondary database, geo-referenced, projected to Universal Transverse Mercator (UTM) and digitized. During the preprocessing exercise, satellite images were rectified for band striping (mis-calibration of the sensor[1]) and cloud cover issues. The study also carried out atmospheric corrections and Landsat calibration to create training sets to extract urban areas specifically from 1990 and 2017 images. The selection of training data in the

[1] Stripping effect is observed in the images when data is loss by sensor while viewing the geometry. Band stripping is caused by miscalibration of sensor either at the detector level or at scan level.

Table 2 Details of datasets at different time stamps for 47 cities of India (climate zone, path and row and satellite name)

S. No.	City name	Climate zone	Image scene 1990	2000	2010	2017
1	Agartala	Warm and Humid	p137r043_5x19911126, p137r044_5x19891104	p137r043_7x20000228, p137r044_7x19991124	LT51370442009315KHC00, LE71370432009083SGS02	LC81360432017058LGN00, LC81360442017058LGN00
2	Agra	Composite	P146R041_5X19891018	P145R042_7X20001001	LT51460412009266KHC00	LE71370432009083SGS02
3	Ahmedabad	Hot and Dry	p149r044_5x19921015, p148r044_5x19901019	p149r044_7x19991027, p148r044_7x20001022	LT51480442009296KHC00, LT51490442009287KHC00	LC81480442017302LGN00
4	Allahabad	Composite	P143R042_5X19901117	P143R042_7X20001120	LT51430422009261KHC00	LC81480382018049LGN00
5	Amritsar	Composite	P149R038_7X19890930	P149R038_7X20010930	LT51480382009296KHC00	LC81480382018049LGN00
6	Asansol	Warm and Humid	P139R043_5X19901121	P139R043_7X20011026	LT51390432009297KHC00	LC81390432018050LGN00
7	Aurangabad	Hot and Dry	p146r046_5x19891018, p139r041_5x19901105	p147r046_7x20001202, p146r046_7x20001024	LT51460462009282KHC00	LC81460462017336LGN00, LC81460472017336LGN00
8	Bengaluru	Temperate	p143r051_5x19910410	p143r051_7x20010224	LT51430512009021BKT00	LC81430512017363LGN00
9	Bhopal	Composite	p145r044_5x19921003	p145r044_7x20001001	LT51450442009003KHC00	LC81450442017041LGN00
10	Chandigarh	Composite	p147r039_5x19891025	p147r039_7x20001015	LT51470392010276KHC00	LC81470392017263LGN00
11	Chennai	Warm and Humid	p142r051_5x19910825	p142r051_7x20001028	LT51420512009046BKT00	LC81420512017084LGN00
12	Dehradun	Composite	146R040_5X19920924	P146R039_7X20001125	LT51470392010276KHC00	LC81460392017080LGN00
13	Delhi	Composite	P146R039_7X19891125	P147R040_7X20000913	LT51460402009298KHC00	LC81470402017087LGN00
14	Dhanbad	Composite	p140r043_5x19921101, p140r044_5x19921101	p139r043_7dk20011026, p140r043_7dk20001014	L71140043_04320091023, L5139044_04420091024	LC81400432017086LGN00, LC81390432017079LGN00
15	Durg	Composite	p142r045_5x19901110, p142r046_5x19901110	p142r045_7x20001215, p142r046_7x20001215	LT51430462009325KHC00, LT51430452009291KHC00	LC81430452017123LGN00, LC81420452017116LGN00
16	Faridabad	Composite	P146R040_7X19891022	P146R040_7X19991022	LT51460402009298KHC00	LC81460412017080LGN00
17	Gangtok	Cold	p139r041_4x19891110	p138r041_7x20011120	LT51380412010021KHC00	LC81400412017070LGN00
18	Ghaziabad	Composite	P146R040_7X19891022	P146R040_7X19991022	LT51460402009298KHC00	LC81460402017096LGN00
19	Guwahati	Cold	P136R042_7X19911219	P136R042_7X19991219	LE71360422009332SGS01	LC81360422017090LGN00
20	Hyderabad	Composite	p144r048_5x19891121	p144r048_7x20011029	LT51440482009300BKT00	LC81430482017091LGN00
21	Indore	Composite	P146R044_7X19991022	147R044_7X20011018	LT51460442009266KHC00	LC81470442017071LGN00
22	Jabalpur	Composite	p144r044_5x19891121	p144r044_7x20001229	L5144044_04420091011	LC81440442017082LGN00
23	Jaipur	Composite	P147R041_5X19891009	P147R041_7X20000913	LT51470412009257KHC00	LC81470412017103LGN00
24	Jodhpur	Hot and Dry	149R042_5X19911029	P149R042_7X20001029	LT51490422009271KHC00	LC81490422017069LGN00
25	Kanpur	Composite	P144R041_5X19891121	P144R041_7X20001111	LT51440422010271KHC00	LC81440422018053LGN00
26	Kochi	Warm and Humid	p144r053_5dt19900124_z43_10	p144r053_7dk20010114_z43_61	LE71440532010039ASN00,	LC81440532016048LGN01
27	Kolkata	Warm and Humid	p138r044_5x19901114	p138r044_7x20001117	LE71380442010301PFS00	LC81390442017079LGN00
28	Kota	Hot and Dry	P147R043_5X19891009	P147R042_7X20000913	LT51470432009257KHC00	LC81460432017064LGN00

Table 2 (continued)

S. No.	City name	Climate zone	Image scene			
			1990	2000	2010	2017
29	Lucknow	Composite	p144r041_5x19891121	p144r041_7x20001111	LT51440412010031KHC00	LC81440412017082LGN00
30	Ludhiana	Composite	P148R038_5X19891016	P148R039_7X20001225	LT51480382009296KHC00	LC81480382017062LGN00
31	Madurai	Warm and Humid	P143R053_5X19900423	P143R053_7X20010515	LT51430532009021BKT00	LC81430542017107LGN00
32	Mumbai	Warm and Humid	p147r047_5x19921204	p147r047_7x19991114	LT51470472009305KHC00	LC81480472017110LGN00
33	Mysuru	Temperate	p144r052_5x19920114	p144r052_7x19991109	LE71440522009020SGS00	LC81440522017114LGN00
34	Nagpur	Composite	P144R045_5X19891105	P144R046_7X20011029	LT51440452009300KHC01	LC81450452017297LGN00
35	Nashik	Hot and Dry	:P147R046_5X19891025	:P147R046_7X20001202	LE71470462009297SGS00	LC81470462017055LGN00
36	Panaji	Warm and Humid	p147r049_5x19891025	p146r050_7x20000314	LE71460492009354SGS0	LC81470492017327LGN00
37	Patna	Composite	P141R042_5X19881012	P141R042_7X20011024	:LT51410422009295KHC00	LC81410422017125LGN00
38	Pune	Warm and Humid	P147R047_5X19921204	P147R047_7X19991114	LT51470472009305KHC00	LC81470472017327LGN00
39	Rajkot	Composite	p150r044_5x19901102	p150r044_7x19991018	LT51500442009294KHC00	LC81500442017364LGN00
40	Shimla	Cold	p147r038_5x19891009	p147r038_7x20001015	LT51470382009305KHC00	LC81470382017103LGN00
41	Srinagar	Cold	p149r036_5x19921015	p149r036_7x20010930	LT51490362009239KHC00	LC81490372017117LGN00
42	Surat	Hot and Dry	p148r045_5x19901019	p148r045_7x20011110	LT51480452009296KHC00	LC81480462017302LGN00
43	Tiruchirapalli	Warm and Humid	p143r053_5x19900423	p143r052_7x20010515	L5143052_05220100209	LC81430522017107LGN00
44	Vadodara	Hot and Dry	P148R044_5X19901019	P148R045_7X20011110	LT51480442009296KHC00	LC81480442017126LGN00
45	Varanasi	Composite	P142R042_5X19901110	P142R042_7X20020204	LT51420422009286KHC00	LC81420422017100LGN00
46	Vasai-Virar	Warm and Humid	P148R047_5X19921109	P148R047_7X20011025	LT51480472009296KHC00	LC81480472017318LGN00
47	Vishakhapatnam	Warm and Humid	P141R048_5X19881012	P141R048_7X20001208	LE71410482009335SGS00	LC81410472017333LGN00

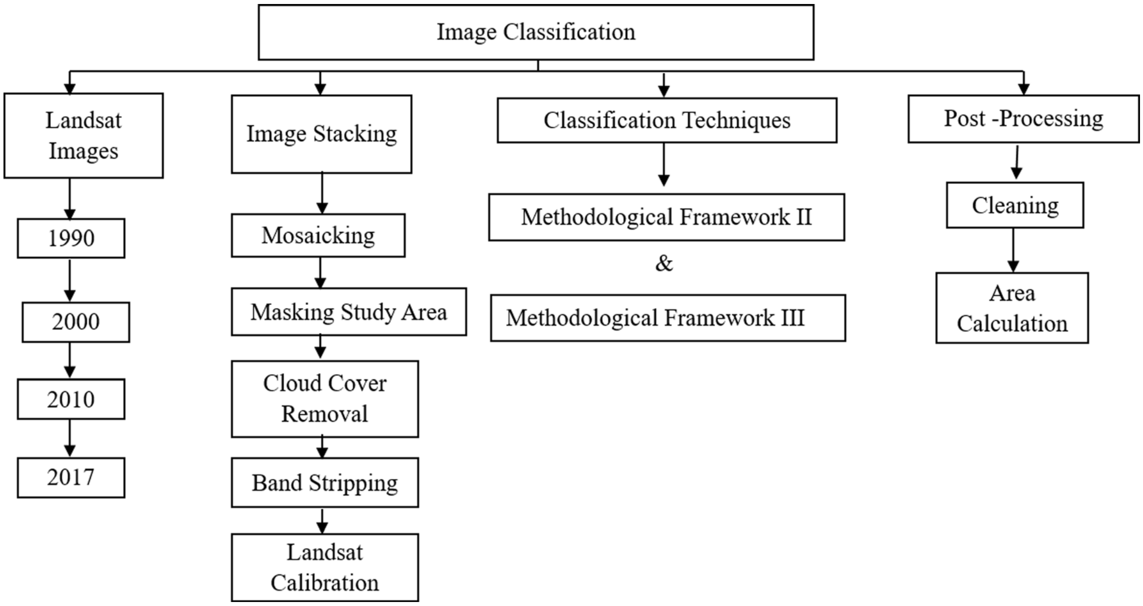

Fig. 1 Methodological framework I

study was based on false color composite (FCC) image, unsupervised classification, top sheet, Bhuvan (ISRO) Web site, and Google™ images.

The classification process was categorized broadly into four stages, i.e., hybrid approach, unsupervised followed by decision tree classification (DTC), and object-based image analysis (OBIA) classification technique, to attain higher accuracy wherever necessary. The initial classification process using hybrid approach for all the 47X4= 188 images reached an average accuracy of 72%. Thus, any image that indicated an accuracy below the average value was considered for improvement in classification techniques. Thus, these images were than further processed using second set of unsupervised classification, or DTC or OBIA or a combination of these approaches. Thus, if accuracy is not reached to 72% level at the hybrid technique stage, then unsupervised classification (ISODATA) approach was used again on problematic classes to improve on the accuracy of classification of LU/LC. If resultant accuracy through hybrid and ISODATA method was not high enough (72%), then DTC was applied to select a set of cities based on the type of classification as explained in Sect. 4.3. The knowledge-based decision tree classification technique used in the study for LU/LC classification as explained in methodological framework II (Fig. 2) helped to further refine the outputs using on normalized difference vegetation index (NDVI). After applying DTC, if results did not match with accuracy criteria or for specific classification errors, the object-based image analysis technique was used for masked problematic classes or subset images to overcome some of the weaknesses of mixed pixel[2] issues as discussed in Sect. 4.4.

Preprocessing

Firstly, all the images (47*4=188) were processed for atmospheric correction employing the cosine of the solar zenith correction (COST) model (Chavez 1996). Out of 47 cities, 17 cities, namely Agartala, Chennai, Dehradun, Delhi, Dhanbad, Durg, Guwahati, Indore, Kochi, Mumbai, Panaji, Shimla, Srinagar, Surat, Trichy, Vasai-Virar, and Visakhapatnam, were processed through Landsat calibration[3] for the years 1990 and 2017 in ENVI.

The Landsat calibration process is based on radiance, reflectance, or brightness temperatures of the image. Landsat bands 5, 6, and 7 represent the short-wave infrared and thermal infrared spectrums of the image having wavelength ranges of 1.55–1.75 µm, 10.40–12.50 µm, and 2.08–2.35 µm, respectively. These bands are useful in identifying moisture of vegetation and soil as well as

[2] A mixed pixel issue occurs when image element signifies properties of more than one surface land cover type. Mixed pixels are found at two concerns, firstly at "edges of large objects" and objects with smaller dimensions for instance agricultural fields, rivers or highways, farms or ponds, or even bushes and trees in sparsely vegetated cover. Secondly appear when imaged objects are smaller in proportion as compared to spatial resolution of the satellite. Landsat TM images reported mixed pixels issues in water 29.6% and 68.3% in vegetation cover (Klein-Gebbinck 1998).

[3] The Landsat calibration refers to procedures that convert from pixel value to radiance value of biophysical cover of the earth surface (Chavez 1989).

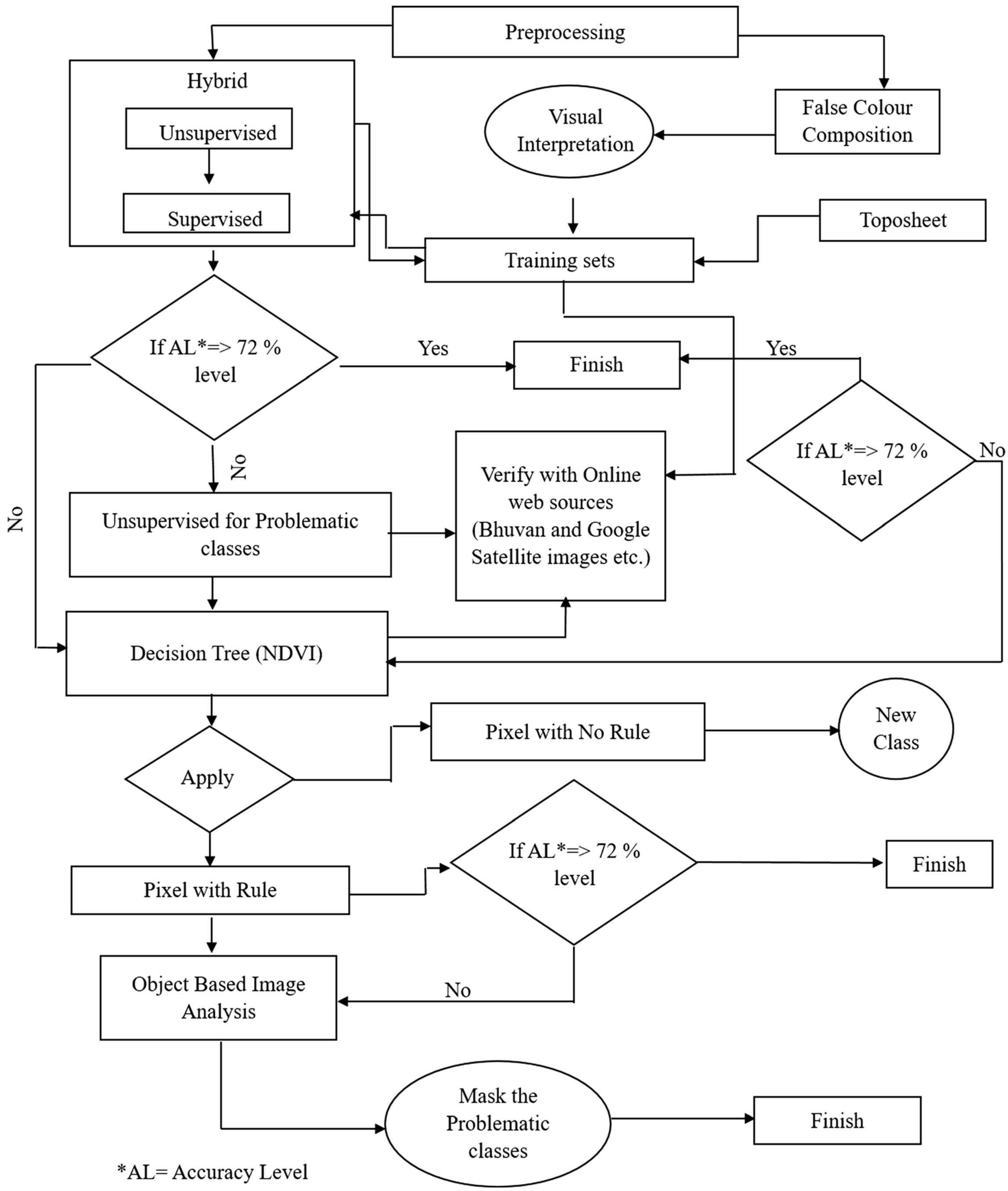

Fig. 2 Methodological framework II

mineral deposits. Thus, this process was supported differentiating spectral signatures of the surface covers like urban built-up, mangrove/swamps/mudflats urban green forest, urban open, mines, saltpans/aqua farms. The classification has been conducted on a stacked image containing all the bands of a Landsat image. It was also applied on Durg and Indore cities, where the urban built-up was underestimated and overestimated, respectively, between 2010 and 2017. One of the possible reasons could be temporal changes in images due to variability in radiometric resolution of Landsat 5 (8-bit data) and Landsat 8 (12-bit data); another reason could be due to image registration[4] issues. Mather and Koch (2011) and Schowengerdt (2006) indicate that similar issues arise while comparing pixel values derived from images in different time frames.

[4] Image registration is the process of transforming datasets into geographic coordinate system acquired from different satellite, sensors, and timeframe.

The de-striping and cloud cover removal process undertaken as a part of the preprocessing affect the spectrum signatures of an image. These processes were required for a couple of images only to be specific—Mysore and Vishakhapatnam cities for de-stripping and Vishakhapatnam and Shimla for cloud cover removal. Once the pixel-based classification was undertaken on these images, the land use classes of the pixels that have undergone preprocessing for de-striping and cloud cover removal were verified using images for same location at different points in time, Google^{TM} images, and secondary data. Mis-classified pixels were manually modified to reflect correct land use class.

As an example, the preprocessing result from Landsat calibration for Kochi City is shown in Fig. 3. Figure 3a shows the before image, while the enhanced results from Landsat calibration in the waterbody, urban area and swamps are depicted in Fig. 3b.

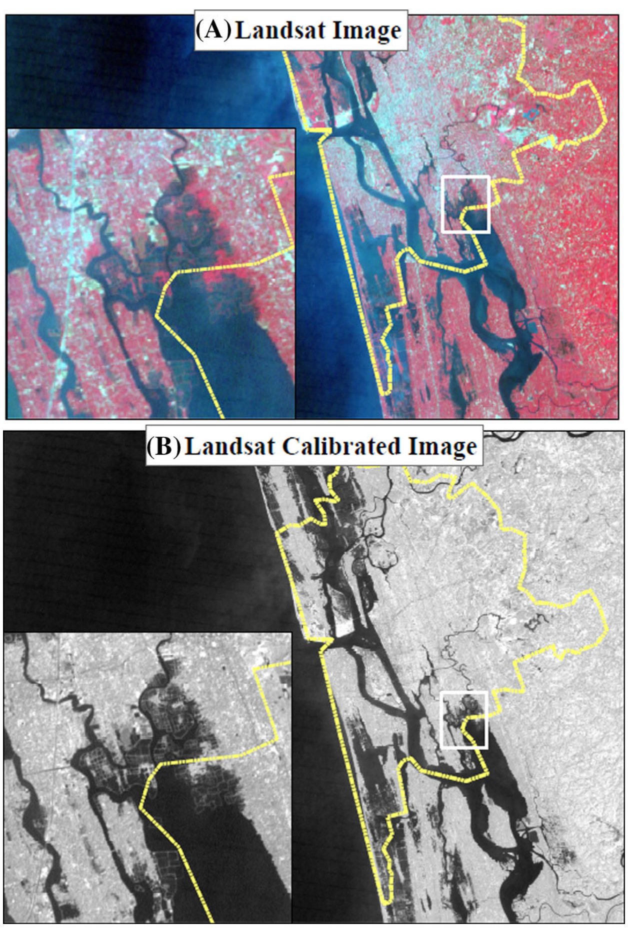

Fig. 3 Landsat calibrated image of Kochi City (2017)

Hybrid Technique

Ground survey plays a significant role in designing training sets, especially to delineate the mudflats, mangroves, and forest. Opting for the traditional ground survey method for 47 cities has its limitations due to time and resource constraints. Some research studies indicate that to attain high accuracy, it becomes essential to use hybrid technique/combination of different techniques that involve multiple levels of classification (Lu and Weng 2007; Campbell and Wynne 2011; Luus et al. 2015; Chen et al. 2017). Hence, the hybrid classification technique which combines supervised and unsupervised classifications has been employed for this study.

Unsupervised

Unsupervised classification method involves minimum human input and doesn't require any previous information of the study area. The unsupervised classification process is a fully data-driven process that allows computer-generated segmentation of satellite image. Distinct clusters or classes are generated depending on spectral responses which are natural grouping based. Every individual pixel is compared to each distinct cluster within the datasets and assigned to the closest cluster with similar spectral values. This study deploys the ISODATA algorithm which classifies images based on the mean value of the class in uniformly distributed data and runs the iteration process using minimum distance technique. In every iteration, it recalculates the mean of the spectral value for each cluster and reclassifies pixels to find a fresh mean until it reaches the maximum number of iterations. Here, 15–18 classes are generated for each image in 10 iterations. This process facilitated to identify LU/LC based on their spectral response.

Supervised

Supervised classification involves the skills of the image analyst to identify training samples from the dataset which characterizes the various themes to be classified (Green et al. 1996). Training sets are referents of the geographical area which represent the particular class on the image. Each class defined within the training set represents a particular LU/LC class (Demir et al. 2014). For this study, we create training sets with the help of images classified using unsupervised processes, Google^{TM} images and secondary data. The ISODATA results for each city and each time period were used to identify the relevant land cover classes based on the spectral signature. These were then used to generate training sets for the relevant land classes for the cities. For example, Panaji being a coastal city had

Table 3 Training sets designed for supervised classification

Individual classes of LU/LC	Description	Training sets
Agriculture	Cultivated land includes plantation, current agricultural fallow areas	4896
Urban Built-up	Area with high–low-rise built-up space includes industrial and commercial built-up spaces	6871
Forest	Large area covered with tree or vegetation defined by Municipal Corporation, Government of India	4211
Urban Open	Land area which currently does not have any vegetation includes open ground and currently fallow	5246
River	A natural stream of water flowing in a upper, middle, and lower course in all decadal years 1990, 2000, 2010, 2017	3760
Bay	A sandy shore area with no vegetation basically land between high- and low-water marks	2115
Swamps/Mangrove	Coastal wetland area with or without vegetation cover	3884
Urban Green	Natural area covered with tree includes parks, green spaces, and natural vegetation	5100
Saltpans/aquafarms	A shallow water manmade container or depression in the ground used for salt industry or aqua industry	1372
Waterbody	Water-filled depression natural or manmade	2679

land cover of saltpans/aquafarms, as well as agriculture, built-up, river, urban green, urban open, and waterbody. Hence, the classes achieved through ISODATA were merged using spectral signatures, Google^{TM} images, and secondary data to generate training sets for 7 classes. Similarly, Jabalpur being a land-locked city, with the presence of forest area, the ISODATA results were used along with Google^{TM} images and secondary data to generate training sets for 6 classes—agriculture, built-up, river, urban green, urban open, waterbody, and forest.

Table 3 provides the details of training sets as per individual classes of LU/LC. Each training set represents sample sites with the digital numbers; these training areas identify each pixel in the satellite images with similar characteristics and classify into the corresponding LU/LC classes. The selection of the appropriate training sets is the key component for success of any supervised classification technique including parallelepiped maximum likelihood, minimum distance, and Mahalanobis distance. The maximum likelihood classifier (MLC) quantitatively calculates both variance and covariance of the class based on its spectral response. MLC assumes that the distribution of a class response is entirely defined by the mean vector and the covariance matrix (Choodarathnakara et al. 2012). It also assumes a normal distribution. The classifier calculates a given pixel's probability of belonging to a particular land cover class (Kantakumar and Neelamsetti 2015).

Liu and Mason (2009) describe that unsupervised classification technique when applied on well-mapped areas may reveal some more classes based on the spectral feature. Hence, after attaining final classes from the hybrid approach, unsupervised classification technique was used again to segregate pixels that were misclassified and to get further segregations in misclassified pixels. For example, the issue of aerosol and atmospheric variability[5] in Dhanbad and Delhi was solved with the help of Landsat calibration and unsupervised technique. The coal mine area of Dhanbad City was misclassified into urban built-up, whereas in Delhi city, a small area of urban built-up and industrial footprint patch was misclassified into water. Similar issues to discriminate more spectral classes in mixed pixels found in Aurangabad, Bangalore, Bhopal, Chandigarh, and Jabalpur cities have been resolved using unsupervised classification technique. A similar process was followed for differentiating waterbodies from rivers since turbid river waters have a higher spectral response when compared to lake waters in the red and infrared components of the spectrum (Duong 2012; Bartolucci et al. 1977). Moreover, feature extraction tool in ENVI 5.4 (object-based identification) was used to differentiate rivers from other waterbodies, for example, river mapping for Agartala as discussed in Sect. 4.4. This process of combining hybrid and unsupervised helped to attain final classification into the land use classes of agriculture, urban built-up, forest, urban open, river, bay, swamps/mangrove, urban green, saltpans, and waterbody. But, some pixels still posed difficulties in achieving classification accuracy. Deployment of MLC under hybrid techniques has major drawbacks in land cover classification since classified classes may not match the spectral response of the image. Thus, DTC was applied with a formula based on the normalized difference vegetation index (NDVI) in such cases.

[5] The signature value of the area is altered by suspension of fine solid or liquid particles in the air. Aerosols can be natural or anthropogenic. Naturally formed aerosols are fog, soil dust, sea salt, volcanoes, botanical debris, forest fires. Direct emission is particulate air pollution and smoke, haze (Lioy and Kneip 1980).

Decision Tree Classification

Decision tree technique is more beneficial when data are ambiguous or inadequate to identity true thematic classes based on their spectral feature in the satellite image (Coppin et al. 2004). Since DTC is a nonparametric method, it helps in classification as well as post-classification processing. DTC has various benefits and is widely used in image processing due to its relatively simple, explicit, and intuitive classification structure (Friedl and Brodley 1997). The construction of DTC requires a set of rules. These rules are designed in a way to solve the purpose of segregating the pixels into land use classes with higher accuracy.

In this study, DTC has been used after running MLC. Misclassified pixels have been rectified after applying knowledge-based decision rule, based on NDVI values and slope function. Pixels classified as agriculture having a slope of greater than 10 degrees (Kantakumar and Neelamsetti 2015) have been converted into the urban green as shown in Fig. 2. Elevation data processed through Shuttle Radar Topography Mission (SRTM) images and Google™ contour data have been used for slope calculations. This slope function is not applied to hilly regions. In hilly regions, wherever there were difficulties in classifying urban green, forest, and agriculture land, DTC was applied on a subset of the image. As discussed by Lee et al. (2011), the threshold values for NDVI have been used as input for the decision tree classification (Lee et al. 2011). NDVI is a widely used indicator to identify land cover types (Yang et al. 2003). Moreover, Hua et al. (2012) suggest use of combined rule of slopes and indices (Hua et al. 2012). Again, as discussed Kantakumar and Neelamsetti (2015) indicate different slopes for different land cover types. Thus, rules combining NDVI and slope have been used in this study for DTC (Fig. 4). These rules were evaluated with the help of literature review, and some of the values are derived from the other field-based research studies (Parthasarathy et al. 2014); details are shown in Table 4. It could be noted that a generalized range has emerged from review of the literature. It has been kept consistent across the analysis in order to maintain consistency of classification process and comparability of classification results. These threshold values range just acts as a guideline for the DTC analysis. Each city has been processed separately for this analysis, and hence, care is taken to ensure that cities with varied geography and location analyzed here are appropriately represented through the land use classes that emerge. For example, an NDVI of say 0.3 in case of Dehradun is expected to not represent mangrove class but rather forest class.

DTC is a tree formed of branches connected with nodes shown in Fig. 4: methodological framework III. DTC values differ as per land use classes and the urban area in focus. The urban green value ranges from 0.12 to 0.26 for hilly regions. Swamps/mangrove value ranges from 0.27 to 0.46, and bay value ranges from − 0.18 to 0 (Parthasarathy et al. 2014) with slope lesser than 5 degrees for coastal areas (shown in Fig. 4). Mangrove/swamps/mudflat and saltpans/aquafarms are also classified with help of visual interpretation techniques based on its appearance in the images. Another example is the shadowing[6] effect (mountain shadow) observed in Dehradun City that has been resolved through a combination of hybrid and DTC approach. However, final results have been verified through specific class-related information available within government documents and Google™ images.

In most of the cases, DTC optimizes maximum overall classification accuracy at the cost of smaller classes (Sharma et al. 2013). Another limitation of DTC faced in this study was its inability to capture details of the river and agriculture land on hilly terrains. Thus, we apply the OBIA technique on such problematic classes as discussed in Sect. 4.4.

Object-Based Image Analysis

Object-based image analysis (OBIA) works on using geographical objects as a key element for identification of LU/LC classification (Dorren et al. 2003; Peña et al. 2014). This approach helps to identify the isolated pixels and misclassified pixels. OBIA recognizes pixels into different types of class depending on its texture, shape, and pattern (Moskal et al. 2011; Hussain et al. 2013; Li et al. 2014). OBIA is a popular methodology among researchers using Landsat MSS, TM, and ETM+ images to detect the urban sprawl; (Kindu et al. 2013; Tewolde and Cabral 2011), vegetation classification (Dorren et al. 2003), waterbody identification (Zhan 2003), and wetlands mapping (Dronova 2015). OBIA works on the principle of segmentation and classification. Post-OBIA processing, the classification accuracy levels for Landsat ETM+ images are reported to be 90% or greater (Phiri and Morgenroth 2017). Amalisana et al. (2017) perform land cover analysis for Bogor, Indonesia, to find that OBIA provided high accuracy results as compared to pixel-based classification (Amalisana et al. 2017). Similarly, Tampubolon et al. (2013) found that OBIA provided reliable classification as compared to traditional maximum likelihood classification for Landsat images of Medan, Sumatera (Tampubolon et al. 2013). Here, segmentation was carried only in problematic situations of identification of area under agriculture for Asansol,

[6] "Shadow occurs when an object totally or partially occludes light directly from the light source. Shadows can be divided into two classes: cast and self" (Arevalo et al. 2005). In remote sensing, shadowing occurs in the images by different objects such as "cloud (cloud shadow), mountain (topographic shadow), and urban material (urban shadow)" (Shahtahmassebi et al. 2013).

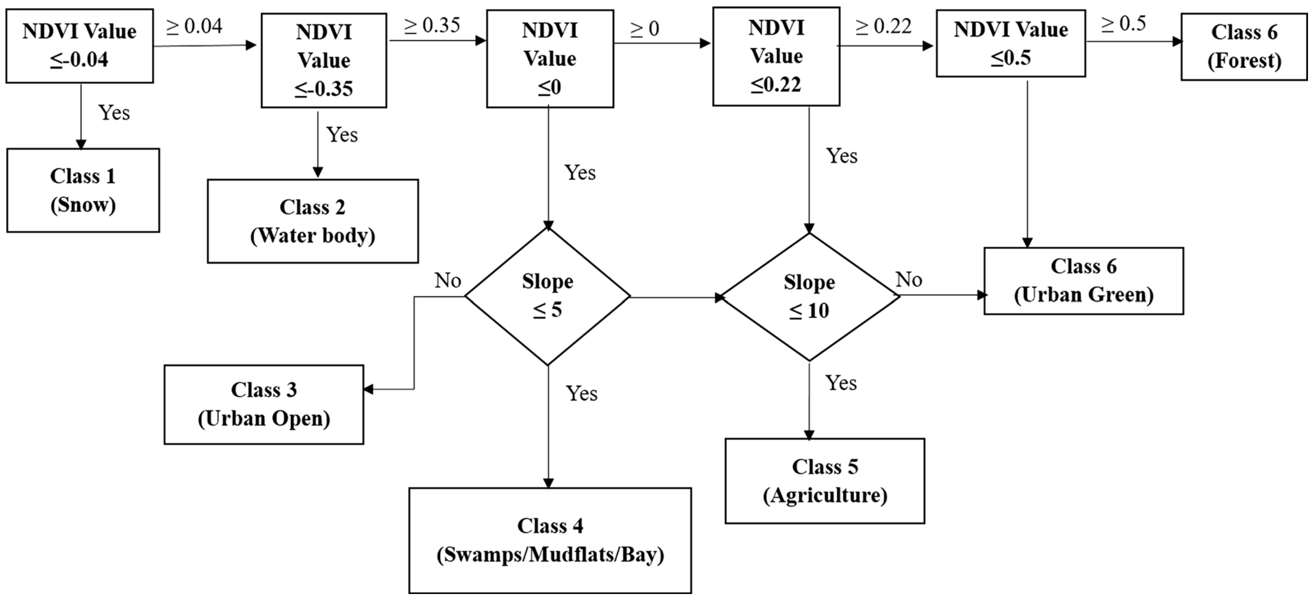

Fig. 4 Methodological framework III for decision tree

Table 4 NDVI value thresholds for various class types

S. No.	Cover type	Value	Source
1	Waterbodies	− 0.06 to − 0.35	Aguilar et al. (2012)
2	Urban green[a]	0.12–0.22	Parthasarathy et al. (2014)
3	Temperate and tropical forest areas#	0.28–0.45	Arulbalaji and Gurugnanam (2014)
4	Dense forest	0.45–0.7	Parthasarathy, et al. (2014)
5	Snow	− 0.046	Holben (1986)
6	Mangrove	0.27–0.46	Guha (2016)

[a]For hilly regions, urban green value ranges between 0.12 and 0.26

Panaji, Gangtok, and Srinagar cities. Firstly, the object's appearance was identified—area under agriculture for Asansol, Panaji, Gangtok, and Srinagar cities on their respective images. The identified pixel sets were then grouped for each of the cities. ENVI 5.4 has been used here for segmentation and classification of these images. In Agartala City, the gorge is steeper at the leeward side of the mountain and average height of region is 13m with undulating topography and low-lying hills; hence, the river has been traced through OBIA technique. The pixels representing river and the hill shadow were separated through segmentation using OBIA, and then, classification was conducted.

Post-processing

In LU/LC classification, results become more valuable when post-processing results resemble actual on-ground features sets. Post-processing performed by integration of multi-level classification processes facilitated in cleaning, merging of datasets (for 1990, 2000, 2010 and 2017) into one layer. This helped in mapping and calculating the decadal change in area under various land use categories. The final datasets are compiled at the city level across the different years; then, the total area was tabulated to create change matrix graph and maps for 47 cities of India. The resultant output has been illustrated through the decadal map for Kochi City shown in Fig. 5. Figure 5 depicts the urban growth of Kochi between 1990 and 2017. Post-processing aids into the validation of accuracy assessment of classified LU/LC results over conventional techniques. The fusion of multi-level classification techniques has helped to attain a high accuracy of multi-temporal datasets. Details of the accuracy assessment are given in the results section.

Results and Discussions

Images Classified Using Different Approaches

LU/LC classification methodology followed here uses a combination of different techniques. It begins with FCC of

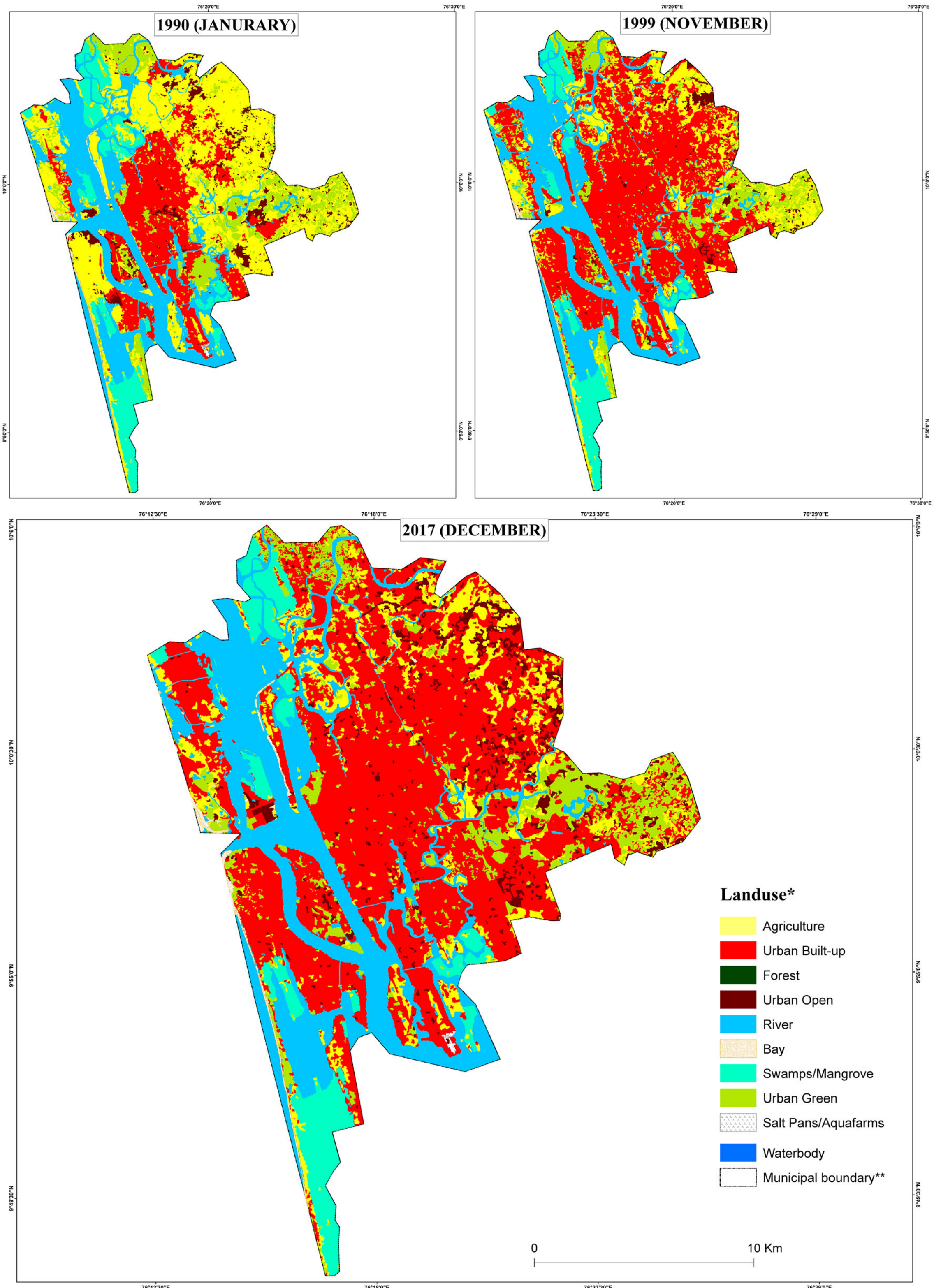

Fig. 5 Land use change map of Kochi City

satellite data, Landsat calibration, hybrid approach in the first step, then applies unsupervised classification technique in the second step, uses of DTC in third stage/step (wherever necessary), and finally uses OBIA in the fourth stage on problematic classes. The DTC-classified maps obtain maximum accuracy in different land use classes and show the best result across all other technique employed. A comparative result illustration for Kochi City, achieved from various techniques, is shown in Fig. 6 ("Appendix 1" describes the land use shares across years for 47 cities).

The Areal Spread of Land Use Classes Under Different Classification Techniques

The total area of the year 2017 (including all 47 cities) as an illustration is calculated for different LU/LC classes under hybrid, DTC, and OBIA techniques (shown in Fig. 7). The total area is calculated in the Universal Transverse Mercator (UTM) projection coordinate system. Agricultural area derived from the hybrid classification process is 3925 km^2, from DTC is 3900 km^2, and through OBIA is 3989 km^2. This increase in the agriculture area under OBIA comes from proper identification and segmentation of agriculture class in the cities of Asansol, Panaji, Gangtok, and Srinagar as discussed in the methods section (4.4). The area under river derived from hybrid classification process is 289 km^2, through DTC is 322 km^2, and using OBIA is 320 km^2. Accuracy of mudflats and saltpans improved from 10.57 km^2 using a hybrid classification approach to 75.03 km^2 by deploying DTC and OBIA. For urban green, the total area accounted for by hybrid classification is 2085.47 km^2, whereas DTC and OBIA accounted for 1550 km^2, indicating that there was overestimation initially. DTC and OBIA classification

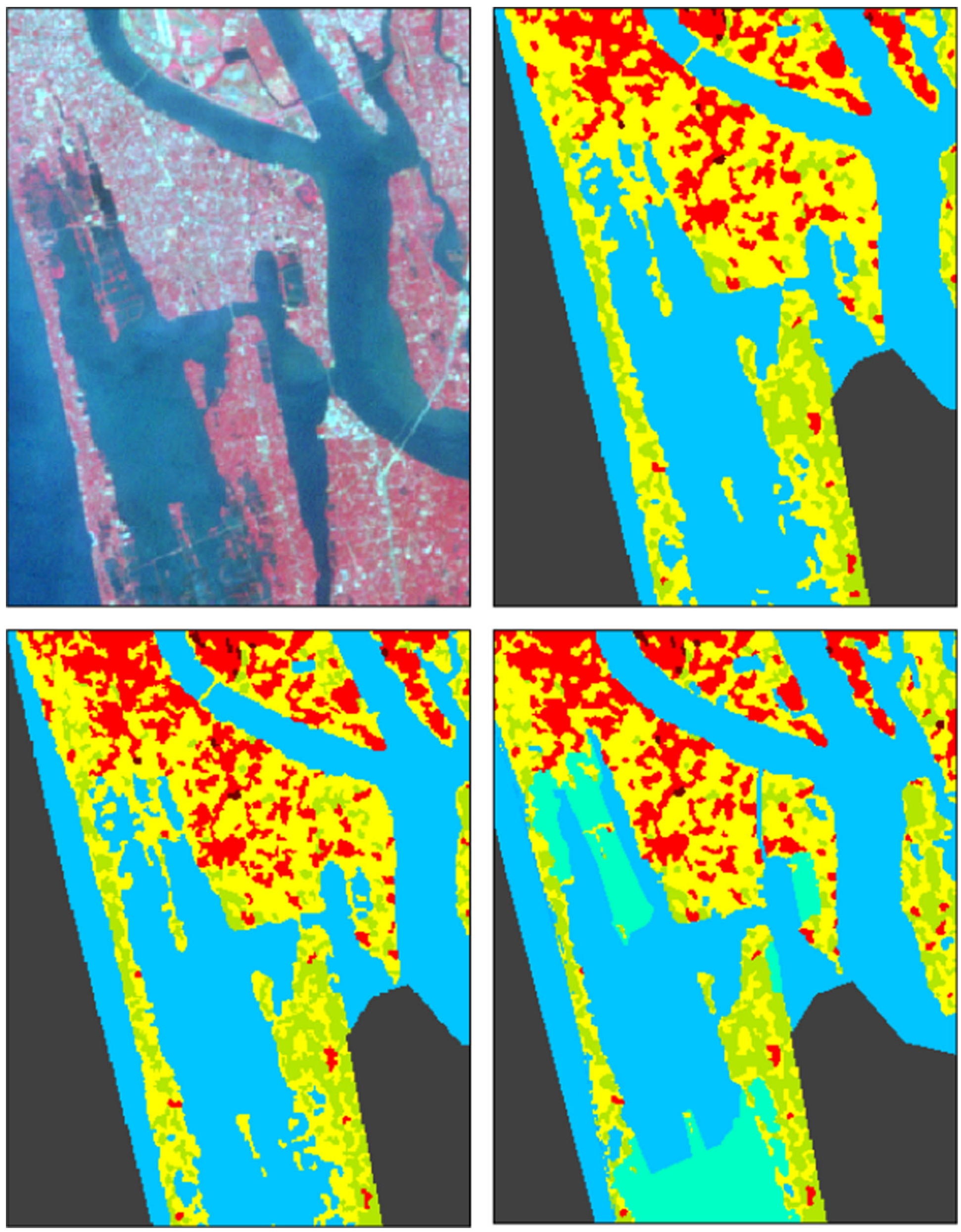

Fig. 6 Classified images with a different approach (snapshots of Kochi City). **a** FCC scheme in Landsat imageries, **b** LU/LC derived from unsupervised classification technique, **c** LU/LC derived from supervised classification technique **d** LU/LC derived from DTC

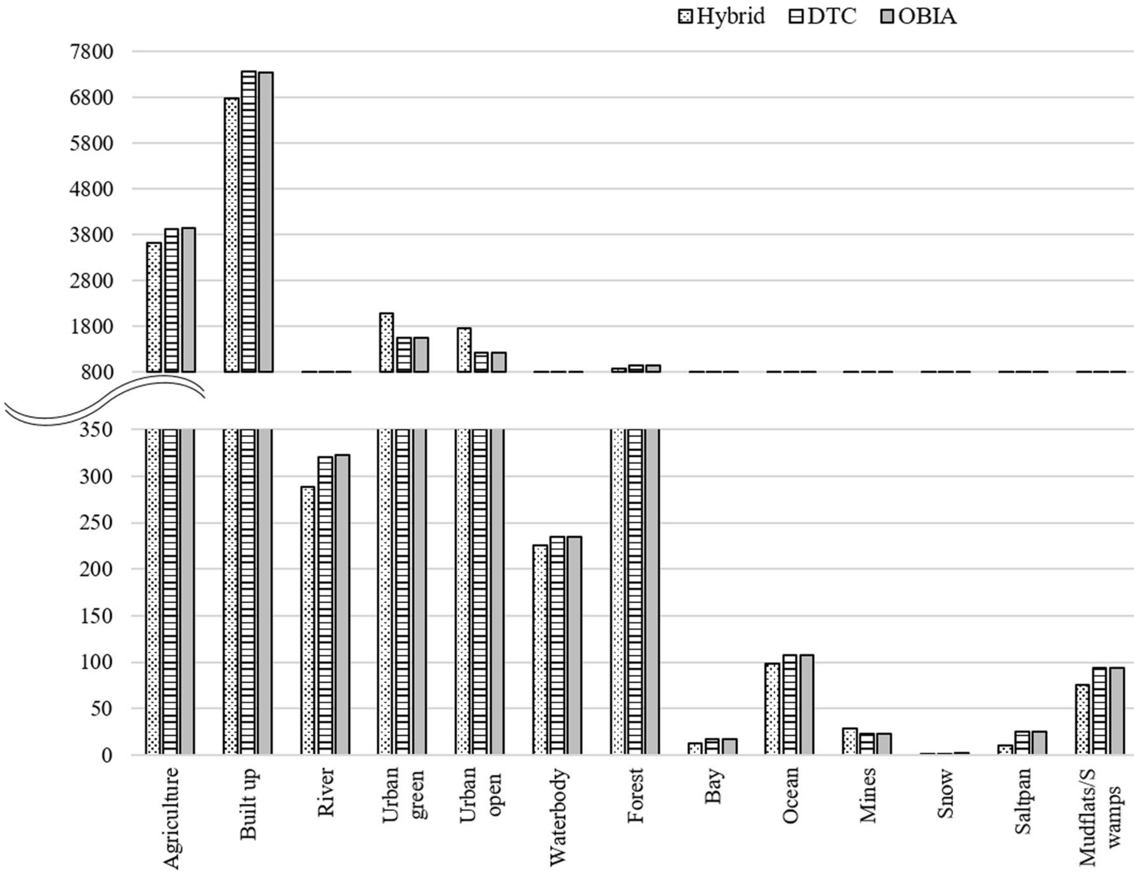

Fig. 7 Total area distribution using different classifiers

processes have increased the classification accuracy for the area under the river, waterbody, saltpan, mudflat, aquafarm and forest (Fig. 7).

Accuracy Assessment

The accuracy of the classification process is evaluated by the error matrix graph. An error matrix that shows several pixels correctly classified into land use classes is the standard method to display the output which validates the accuracy of final results. In Table 5, Kochi City has been used for illustration of accuracy assessment of unsupervised, supervised, and DTC techniques ("Appendix 2" describes the accuracy assessment details for all the 47 cities). The purpose is to show variations observed in classification results by traditional methods versus DTC. For Kochi, DTC gave the best results with an overall accuracy of 90.14% and kappa coefficient of 0.89 as compared to hybrid classification at 78.96% overall accuracy and 0.75 kappa coefficient value. This result illustrates the advantages of the adoption and development of multiple classification techniques in the study region.

There are several factors that confuse the spectral signature of the images, including topography, shadowing, atmospheric variability, sensor calibration, and class mixing instantaneous field of view (IFOV) (Choodarathnakara et al. 2012; Wang and Chen 2012). In this study, we have experienced different issues; details are reported in Table 6. It describes details of issues faced during processing due variability of spectral signatures and the respective resolution of the issue through applying different basket of techniques at various stages on cities to improve the classification accuracy. It can be observed that the overall accuracy of classification among the cities ranges from 81 to 93% and the kappa coefficient varies from 0.76 to 0.91.

Discussion

There have been several advances in the field of remote sensing and satellite data processing in the recent years (Garg et al. 2018)—improving the efficiency of image classification process being one of them. Recent studies describe methods that aim at achieving higher accuracies (Mandal et al. 2019; Nazmfar and Jafarzadeh 2018). Through this study, we demonstrate an approach of combining various classification techniques (parametric as well as nonparametric) in order to improve the classification

Table 5 Accuracy assessment of three techniques (in percentage) for Kochi. *Source*: Author's estimations

Classes	Unsupervised		Supervised		Hybrid		DTC	
	UA	PA	UA	PA	UA	PA	UA	PA
Agriculture	58.48	54.05	69.44	67.11	77.52	71.94	84.75	96.15
Urban built-up	56.03	43.33	67.71	71.43	92.86	74.71	92.86	87.84
Urban green	42.50	42.50	61.26	62.96	69.39	80.95	87.18	79.07
Urban open	37.16	43.65	59.14	61.80	62.50	74.32	90.16	87.30
Mudflats/mangrove	52.67	37.70	71.88	54.33	77.53	68.32	89.61	94.52
Bay	53.85	38.25	77.78	59.83	87.50	70.71	88.61	80.46
River	55.56	42.25	78.95	68.18	81.08	84.51	93.75	96.77
Waterbody	50.96	42.55	76.92	62.02	88.89	70.18	97.56	95.24
Saltpan/aquafarms	47.17	39.47	70.75	64.66	78.95	60.48	92.59	93.75
	OA = 50.15	K =0.43	OA =70.08	K = 0.66	OA=78.96	KA= 0.75	OA = 90.14	K = 0.89

Landsat calibration+ hybrid+ DTC*

UA, user's accuracy; PA, producer's accuracy; OA, overall accuracy; K, kappa statistics

accuracies and derive high-quality land use land cover data for urban areas. In order to bring in comparable results, the methodology followed here has also been kept consistent. Recent studies on land use land cover classification of Indian cities are generally limited a single city or a region around a city (Meer and Mishra 2020; Mandal et al. 2019; Ramachandran and Reddy 2017; Vaz et al. 2017). The robustness of the methodology adopted here has been demonstrated through use of 47 urban areas across India with cities falling under different sizes, climate zones, and geographies ranging from Himalayan cities to coastal cities, arid cities of Rajasthan, and land-locked cities in warm and humid parts of India as well as 4 time points in the history.

Also to note here is that the study does not include ground truthing in its traditional sense of collecting GPS points across all cities. One of the limitations here is that the spatial resolution of 30 $\times$ 30 m of Landsat images may not be sufficient for analyzing finer details. The study explores cities falling under different geographies, where one technique imparted on a city may not be successfully imparted in the other city. However, results derived from the accuracy assessment are promising, thus encouraging further development and methodological implications of multiple classification techniques for achieving higher classification accuracies across urban areas located in varied geographies.

Conclusion

The selection of classification techniques in remote sensing studies is highly dependent on the purpose of the research study, the classification level selected, and the timeline considered for the study. For this study on 47 cities across four time points, we started with traditional classification methods such as supervised and unsupervised techniques. The results obtained proved to be unsatisfactory in terms of their accuracy achieved in the case of several cities. Thus, this study employs multiple classification techniques on the processed data to achieve results with higher classification accuracy—the most prominent being hybrid classification. Hybrid classification technique, which encompasses the advantages of both the supervised and unsupervised classification methods, provided significant improvement in accuracy results for multi-temporal datasets. Hence, for 14 cities out of 47 cities, the classification accuracy requirement of 72% was achieved in hybrid classification. For problematic classes, we used DTC, OBIA, and unsupervised classification techniques after masking the datasets. DTC was used in cities with more number of problem in datasets. DTC approach was designed after an extensive literature review and some of the field expertise on land use and coastal mapping. DTC provided with the improvement in classification accuracy over the hybrid approach. The results show an overall accuracy of 90%, and the developed classification technique was successful in differentiating green cover with accuracy level greater than 75%. This was a marked increase in accuracy over the hybrid approach where natural vegetation classes overlapped with each other and were hard to distinguish.

Table 6 Details of issues, technique deployed, and accuracy assessment

S. No.	Cities	Observed concerns	Issue	Resolved	Basket of techniques deployed	Accuracy	
						Overall (%)	Kappa coefficient
1	Agartala	Difficulties to map the river, gorge is steeper at leeward side of mountain (average height of region is 13m with undulating topography and low-lying hills)	Topography (river tracing)	Pattern recognition (OBIA)	Landsat calibration + hybrid + unsupervised + OBIA	91.92	0.90
2	Agra	Difficulties in identification of forest and urban green inside the city	Mixed pixel	DTC	Hybrid + DTC	91.63	0.90
3	Ahmedabad	Urban open misclassified into urban built-up	Mixed pixel	DTC	Hybrid + DTC	90.06	0.88
4	Allahabad	N.A	–	–	Hybrid	90.23	0.88
5	Amritsar	N.A	–	–	Hybrid	92.1	0.90
6	Asansol	The agricultural farms are very small in size in this region, and they were inseparable with urban green	Mixed pixel	Pattern recognition (OBIA)	DTC + OBIA	91.15	0.89
7	Aurangabad	Agriculture pixels were misclassified into urban open and urban green	Mixed pixel	Unsupervised	Hybrid + unsupervised	91.81	0.90
8	Bangalore	Urban open misclassified into urban built-up	Mixed pixel	Unsupervised	Hybrid + unsupervised	88.89	0.87
9	Bhopal	Urban open misclassified into urban built-up	Mixed pixel	Unsupervised	Hybrid + unsupervised	92.66	0.91
10	Chandigarh	Difficulties faced between demarcation of forest and urban green	Mixed pixel	Unsupervised	Hybrid + unsupervised	91.62	0.90
11	Chennai	Bay misclassified into waterbody	Mixed pixel	Landsat calibration and DTC	Landsat calibration + hybrid + DTC	88.4	0.87
12	Dehradun	Forest, urban built-up, and river misclassified	Mixed pixel and shadowing (mountain shadow)	Landsat calibration and DTC	Landsat calibration + hybrid + DTC	89.01	0.87
13	Delhi	Urban built-up (specifically industrial) area misclassified to urban open	Aerosol and atmospheric variability	Landsat calibration and unsupervised	Landsat calibration + hybrid + unsupervised	88.84	0.87
14	Dhanbad	Mines misclassified into urban open and waterbody	Aerosol and Atmospheric variability	Landsat calibration and unsupervised	Landsat calibration + hybrid + unsupervised	91.09	0.90
15	Durg	The total urban built-up area for 2010 was under estimated, and it was correctly estimated in 2017	Calibration changes (feature enhancement)/image registration (geo-correction)	Landsat calibration and unsupervised	Landsat calibration + hybrid + unsupervised	91.97	0.90
16	Faridabad	Forest and waterbody (specifically at edges of canal) misclassified	Mixed pixel	DTC	Hybrid + DTC	90.25	0.89

Table 6 (continued)

S. No.	Cities	Observed concerns	Issue	Resolved	Basket of techniques deployed	Accuracy	
						Overall (%)	Kappa coefficient
17	Gangtok	Forest and agricultural misclassified	Mixed pixel and Topography (River tracing)	Pattern recognition (OBIA)	Hybrid + DTC + OBIA	88.55	0.87
18	Ghaziabad	N.A	–	–	Hybrid	91.03	0.89
19	Guwahati	Unable to capture small waterbody in 1990	Calibration changes (feature enhancement)	Landsat calibration and DTC	Landsat calibration + hybrid + DTC	91.75	0.90
20	Hyderabad	Urban green misclassified into agriculture and urban open	Mixed pixel	DTC	Hybrid + DTC	87.29	0.85
21	Indore	The total urban built-up area for 2017 was under estimated, and it was correctly estimated in 2010	Calibration changes (feature enhancement)/image registration (geo-correction)	Landsat calibration and unsupervised	Landsat calibration + hybrid + unsupervised	91.54	0.89
22	Jabalpur	Small waterbody misclassified into urban built-up	Mixed pixel	Unsupervised	Hybrid + unsupervised	90.94	0.89
23	Jaipur	N.A	–	–	Hybrid	87.37	0.85
24	Jodhpur	N.A	–	–	Hybrid	90.61	0.89
25	Kanpur	N.A	–	–	Hybrid	87.2	0.84
26	Kochi	Urban built-up misclassified into green. Swamps/Mangrove was misclassified into waterbody and urban green	Mixed pixel	Landsat calibration and DTC	Landsat calibration + hybrid + DTC	90.01	0.88
27	Kolkata	Urban green was misclassified into urban built-up. Difficulties in delineation of boundary of waterbody	Mixed pixel	DTC	Hybrid + DTC	88.98	0.86
28	Kota	N.A	–	–	Hybrid	89.88	0.88
29	Lucknow	N.A	–	–	Hybrid	91.25	0.88
30	Ludhiana	N.A	–	–	Hybrid	92.92	0.91
31	Madurai	The area under urban open and waterbody in 1990 (difficulties faced in extraction of waterbody)	Mixed pixel (because of seasonal variability of Images)	DTC	Hybrid + DTC	92	0.90
32	Mumbai	Difficulties in identification of Swamps, saltpans and river	Mixed pixel	Landsat Calibration and DTC	Landsat calibration + Hybrid + DTC	90.4	0.89
33	Mysore	Band striping	Miscalibration of sensor	Destripe	Destripe + hybrid + DTC	90.2	0.88
34	Nagpur	N.A	–	–	Hybrid	90.34	0.88
35	Nasik	N.A	–	–	Hybrid	91.82	0.90

Table 6 (continued)

S. No.	Cities	Observed concerns	Issue	Resolved	Basket of techniques deployed	Accuracy	
						Overall (%)	Kappa coefficient
36	Panaji	Difficulties in distinguishing between saltpans and swamps/mudflats	Mixed pixel	DTC and pattern recognition (OBIA)	Landsat calibration + hybrid + DTC + OBIA	90.83	0.90
37	Patna	Difficulties in extraction of urban built-up, urban green and agricultural land near River Ganges	Mixed pixel	DTC	Hybrid + DTC	90.16	0.88
38	Pune	Difficulties in extraction of forest and urban green	Mixed pixel	DTC	Hybrid + DTC	93.98	0.93
39	Rajkot	Band striping	Miscalibration of sensor	Destripe	Destripe + hybrid	89.94	0.90
40	Shimla	Difficulties faced in identification and separation of agriculture and forest	Mixed pixel	Landsat calibration and DTC	Landsat calibration + hybrid + DTC	87.95	0.88
41	Srinagar	Difficulties faced in identification and separation of agriculture and forest	Mixed pixel	Landsat calibration and DTC	Landsat calibration + hybrid + DTC + OBIA	89.69	0.90
42	Surat	Difficulties faced in identification, mudflats and saltpans	Mixed pixel	Landsat calibration and DTC	Landsat calibration + hybrid + DTC	91.85	0.91
43	Trichy	Difficulties faced in identification of urban open and waterbody	Mixed pixel	Landsat calibration and DTC	Landsat calibration + hybrid + DTC	92.24	0.92
44	Vadodara	N.A	–	–	Hybrid	91.93	0.92
45	Varanasi	N.A	–	–	Hybrid	90.84	0.89
46	Vasai-Virar	Difficulties faced in identification of swamps/mangrove and urban green	Mixed pixel	Landsat calibration and DTC	Landsat calibration + Hybrid + DTC	90.24	0.89
47	Visakhapatnam	Difficulties in delineation of waterbody, bay and urban built-up (Industrial) at the coast	Aerosol and atmospheric variability	Landsat calibration and DTC	Landsat calibration + hybrid + DTC	81.125	0.77

The purpose of this paper is to demonstrate the use of a combination of multiple classification techniques to achieve higher classification accuracy for multi-temporal, multi-city datasets. This paper concludes that a combination of multi-level classification techniques has improved performance in terms of classification accuracy levels for urban areas. This technique is inclusive of different techniques and thus makes it a unique approach for land use classification. Results show improvement in the accuracy of agriculture and green in hilly regions, swamps and salt pans in the coastal cities. As an example of coastal (Kochi) city with eleven different types of LU/LC classes, the accuracy levels obtained were reported to be 51% for unsupervised classification. Supervised classification and DTC enhanced it to 77% and further to 90%, respectively.

Acknowledgements This research study was partly funded by the Indo-Norwegian Cooperation Project (INCP-2014/10093), as well as DDP Initiative (ddpinitiative.org) and the International Climate Initiative (IKI) (18_I_326_Global_A_Climate Action After Paris). INCP was jointly undertaken by the Governments of India and Norway through University Grants Commission (UGC) India and The Norwegian Centre for International Cooperation in Education (SIU). The Federal Ministry for the Environment, Nature Conservation and Nuclear Safety (BMU) supports the DDP initiative on the basis of a decision adopted by the German Bundestag under the project titled "From NDCs to Pathways and Policies: Transformative Climate Action After Paris."

Appendix 1: Land Use Shares for 47 Cities for 1990, 2000, 2010, and 2017

Agartala

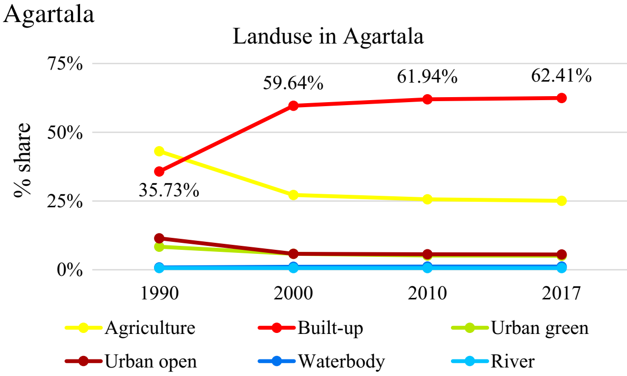

Agra

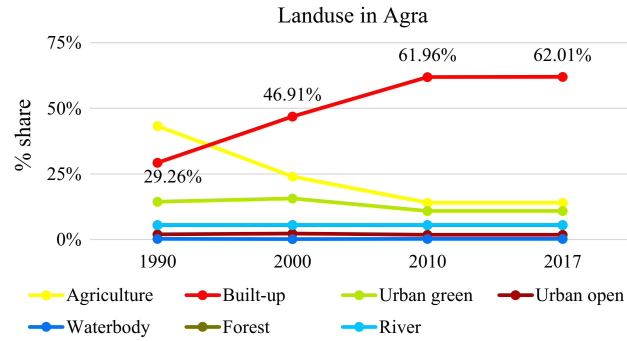

Ahmedabad

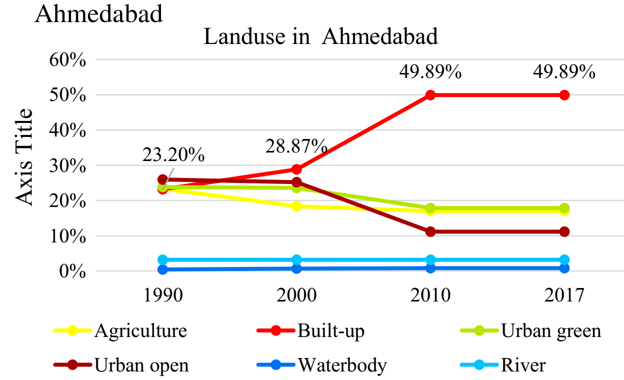

Allahabad

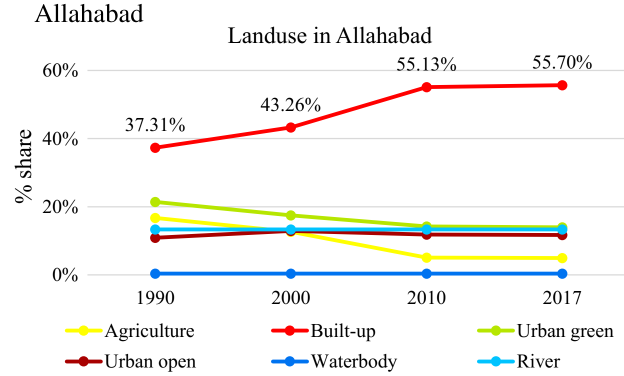

Amritsar

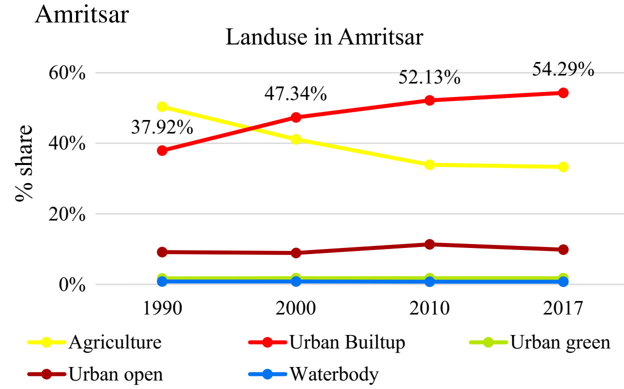

Asansol

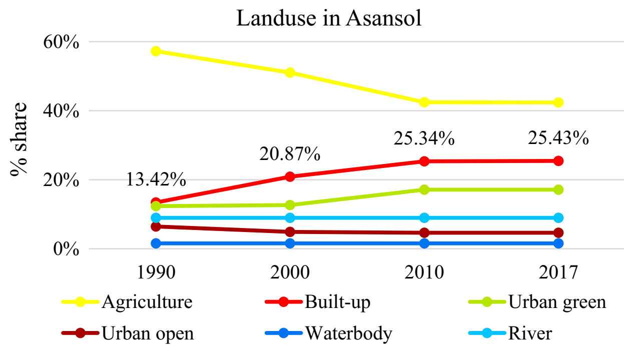

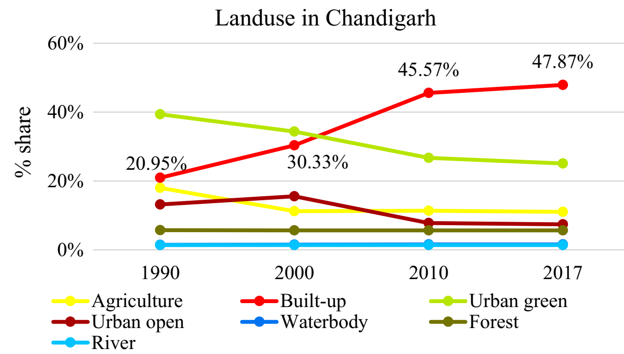

Aurangabad

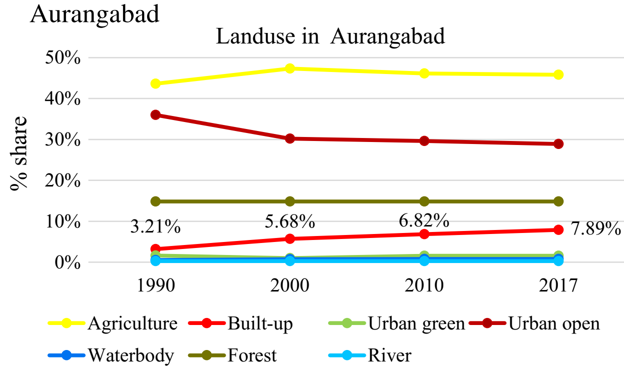

Chennai

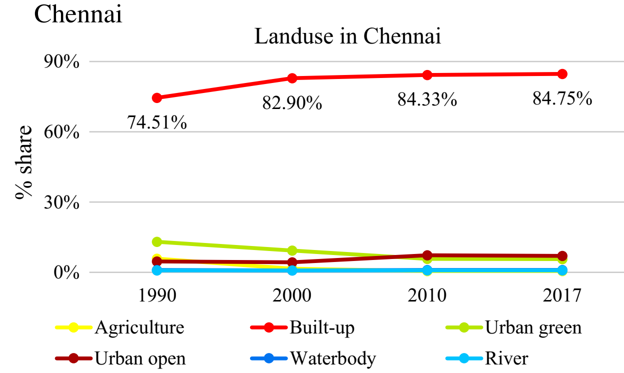

Bengaluru

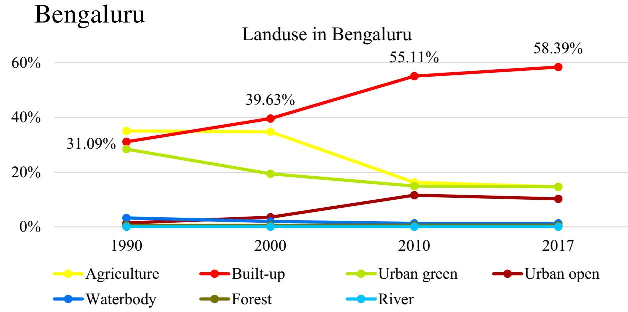

Dehradun

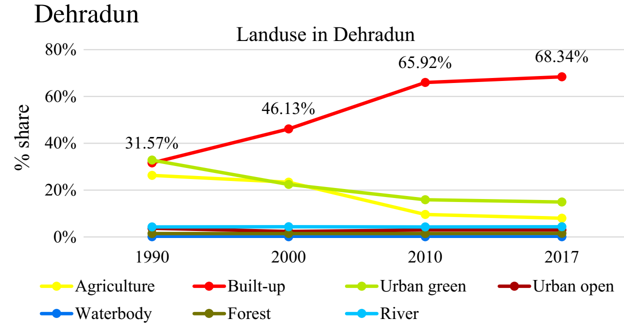

Bhopal

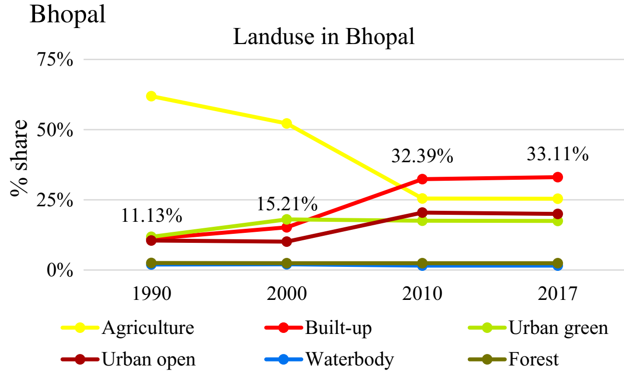

Delhi

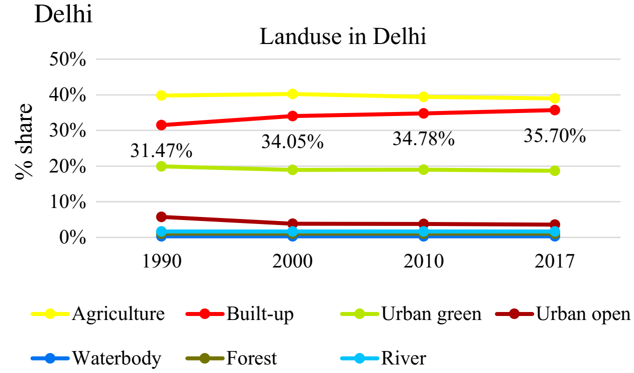

Chandigarh

Dhanbad

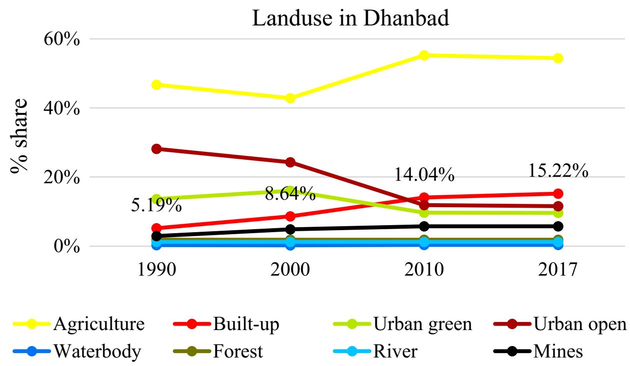

Durg-Bhilainagar

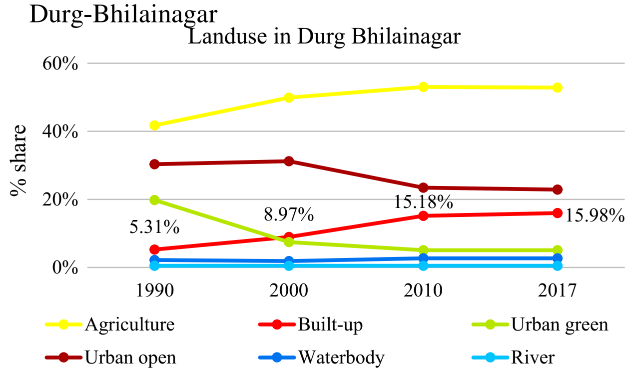

Faridabad

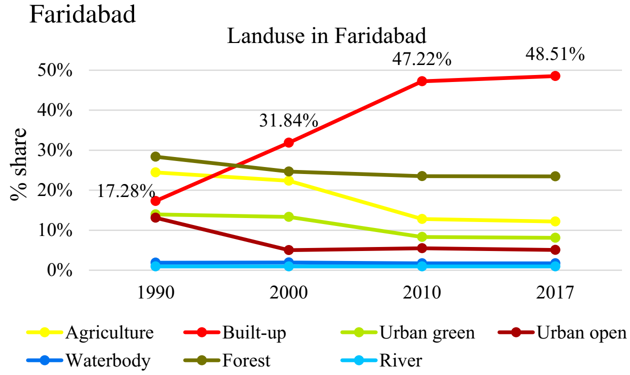

Gangtok

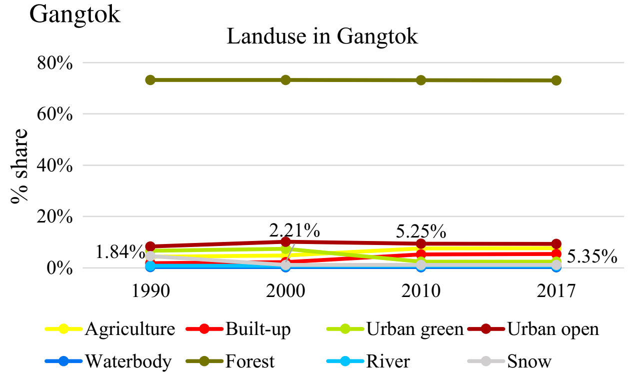

Ghaziabad

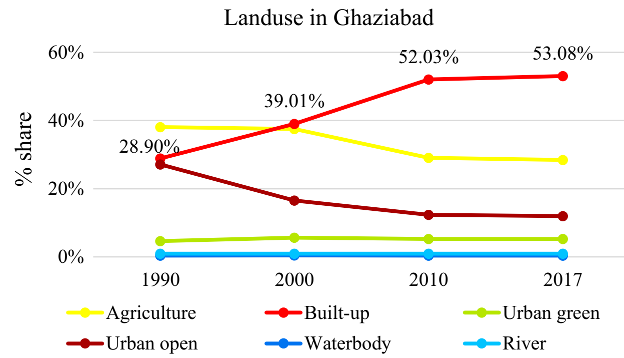

Guwahati

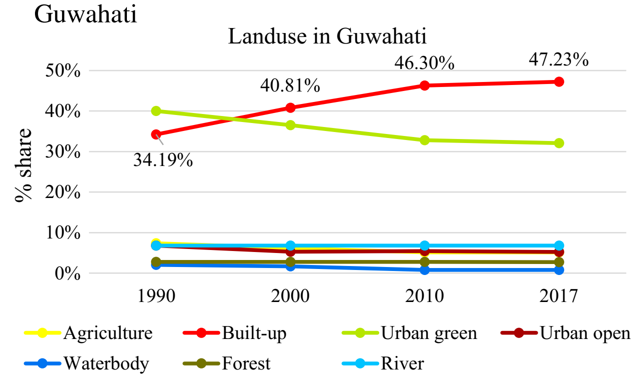

Hyderabad

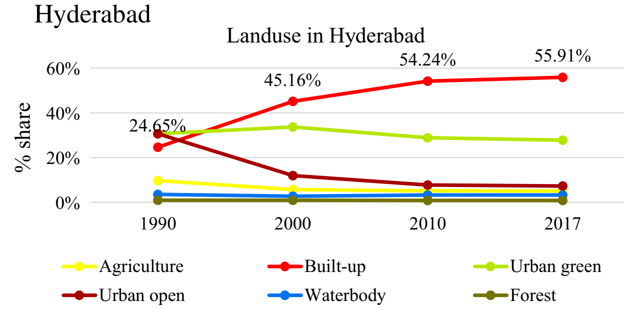

Indore

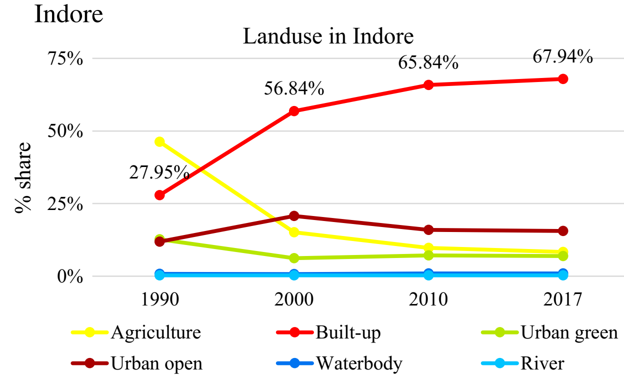

Jabalpur

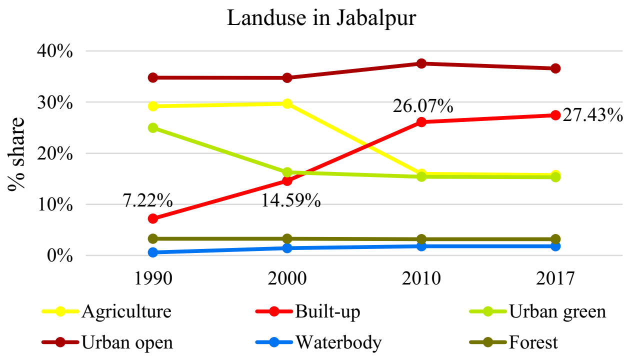

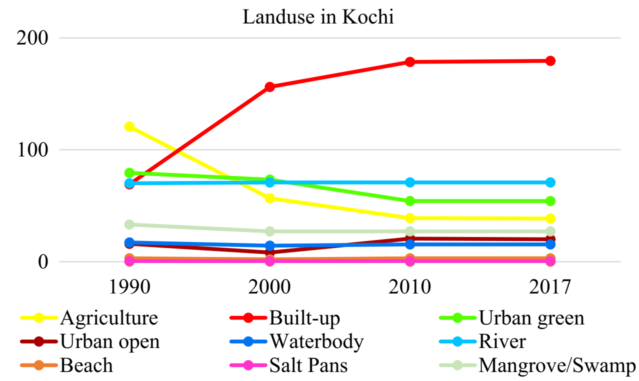

Jaipur

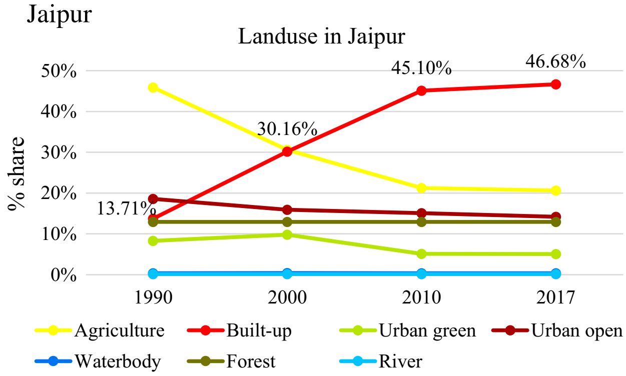

Kolkata

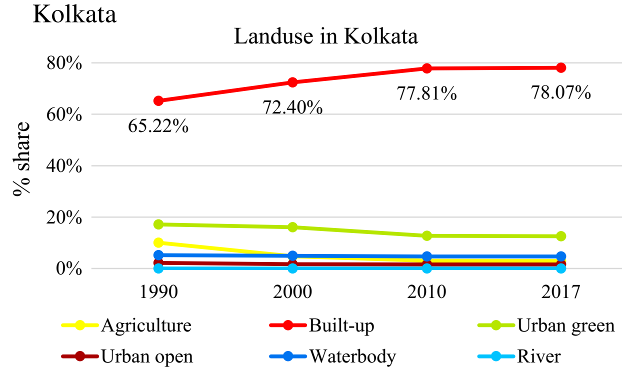

Jodhpur

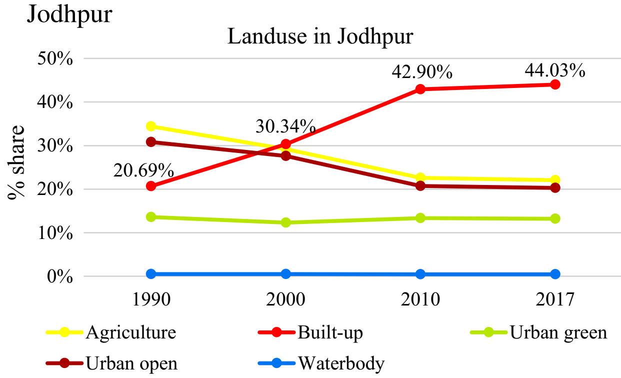

Kota

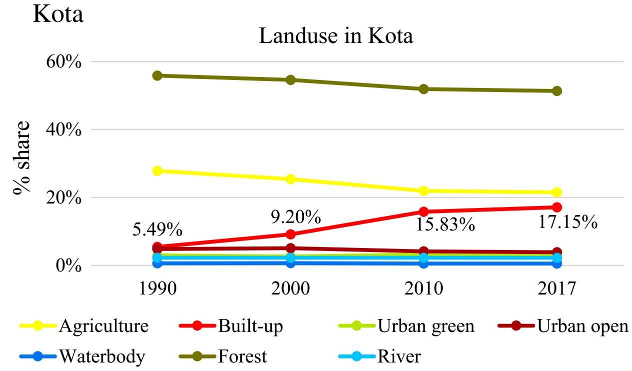

Kanpur

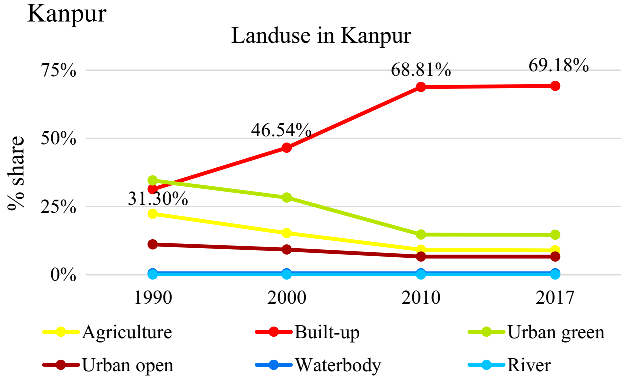

Lucknow

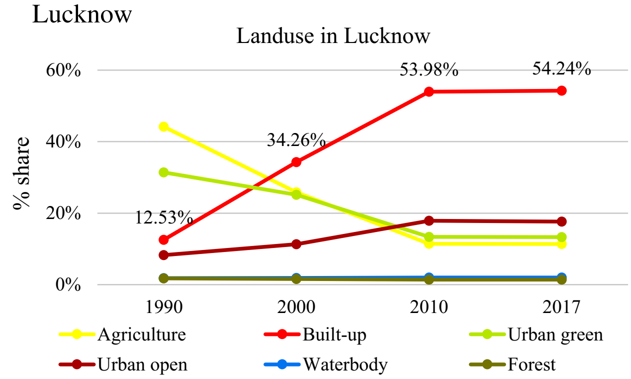

Kochi

Ludhiana

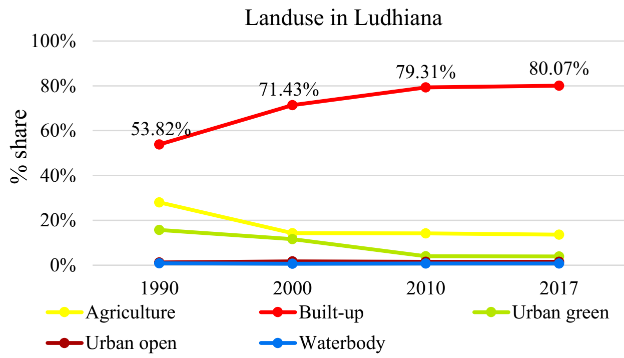

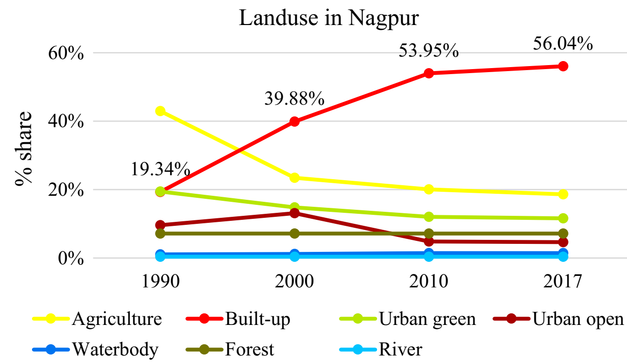

Madurai

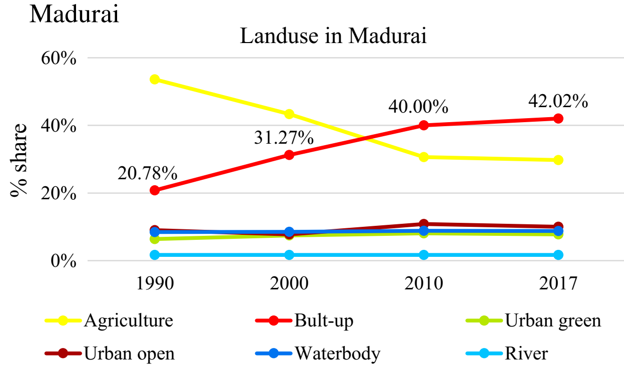

Nashik

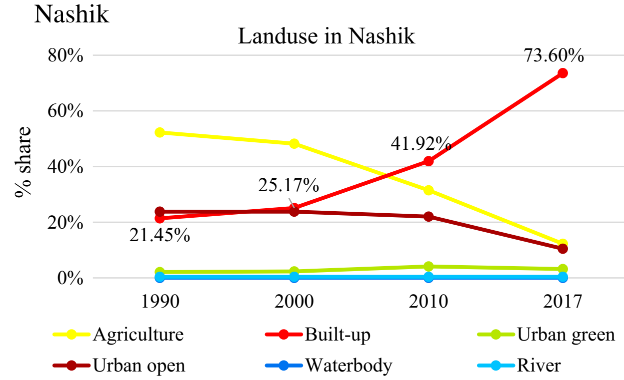

Mumbai

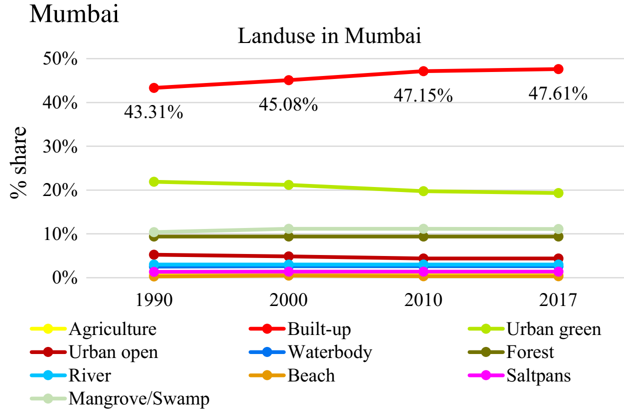

Panaji

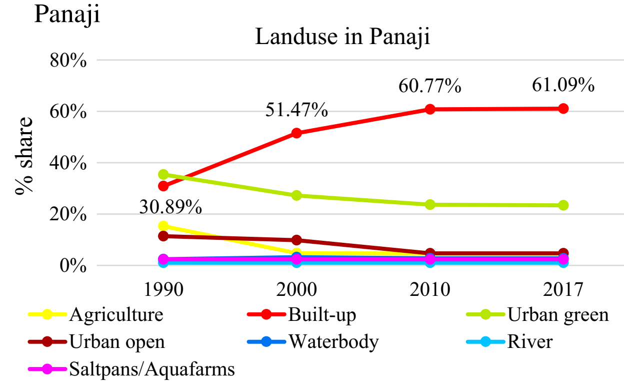

Mysuru

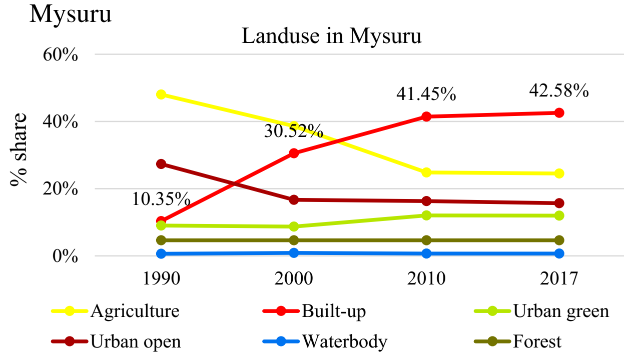

Patna

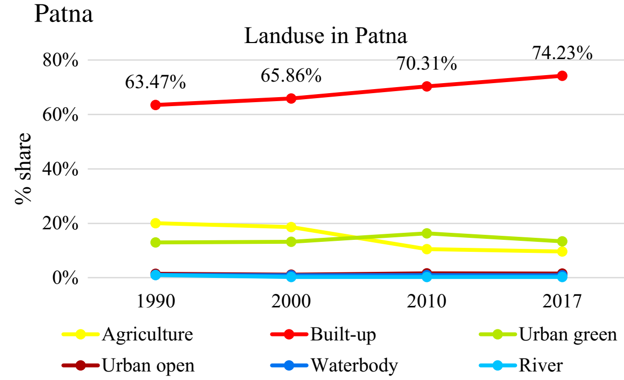

Nagpur

Pune

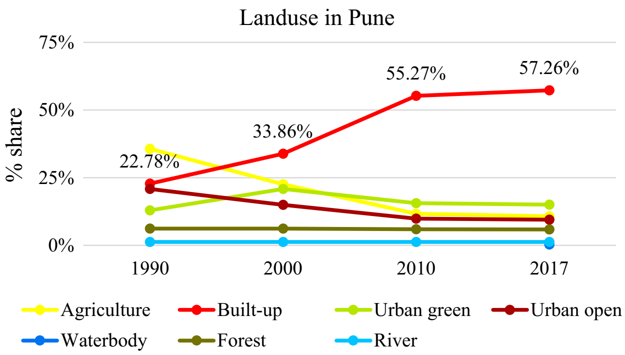

Rajkot

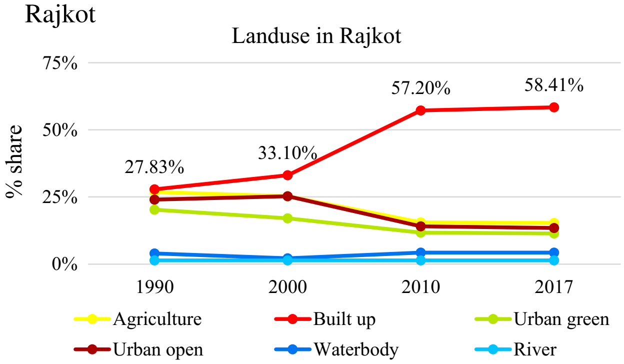

Shimla

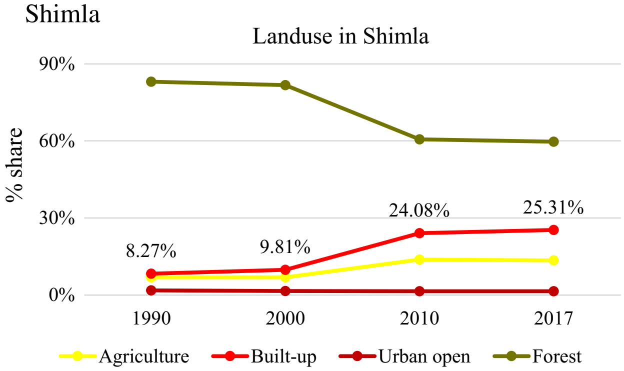

Srinagar

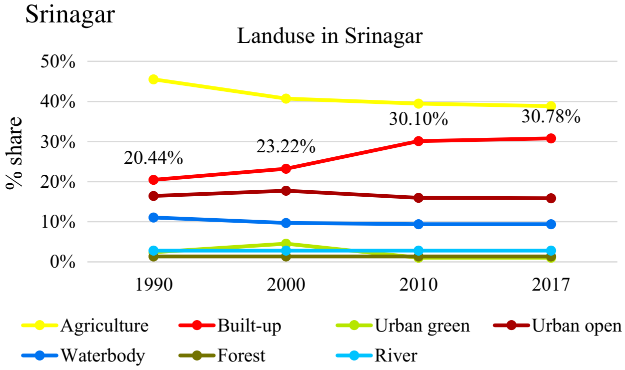

Surat

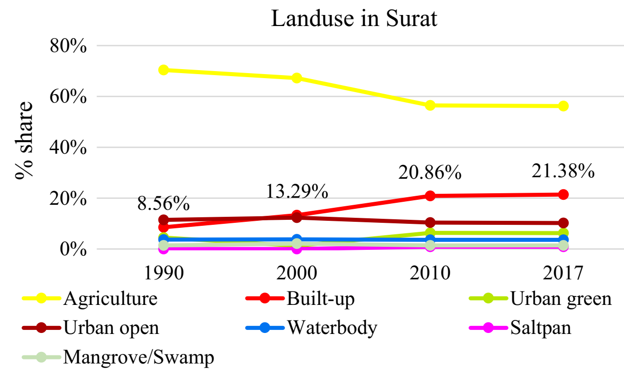

Tiruchirapalli

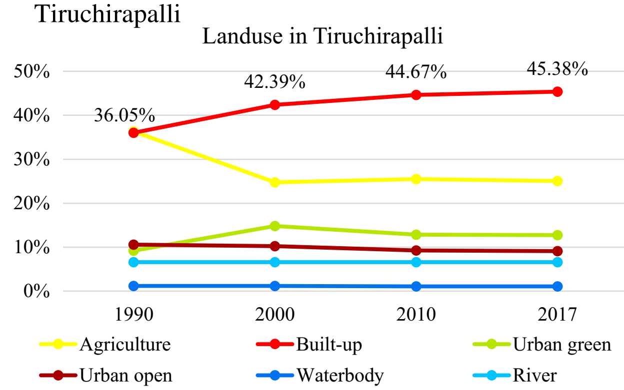

Vadodara

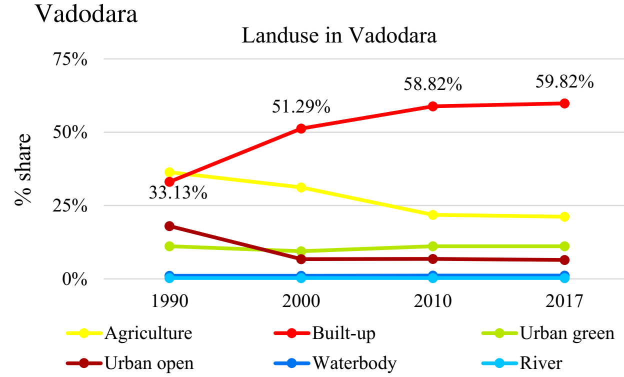

Varanasi

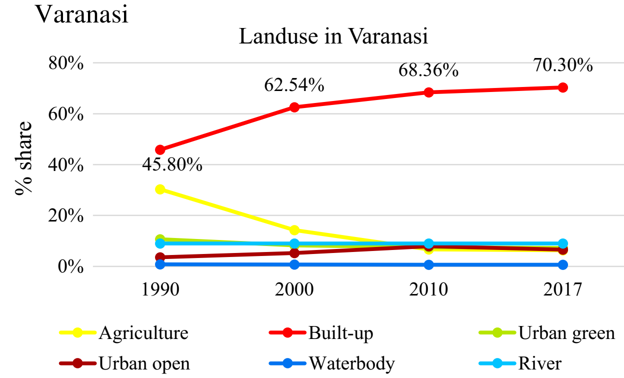

Vasai-Virar

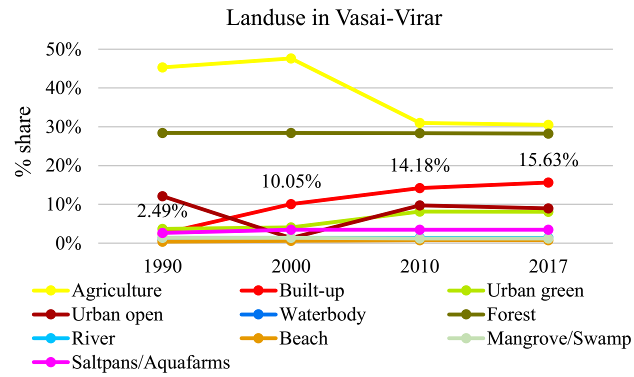

Vishakhapatnam

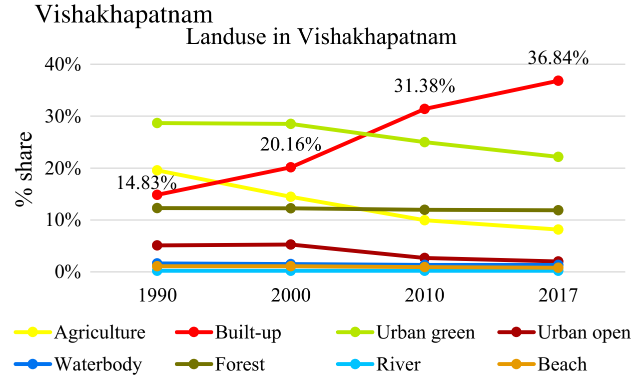

Appendix 2: Accuracy Assessment for all 47 Cities

S. No.	Cities	Accuracy (in percentage)		
		Classes	User	Producer
1	Agartala	Agriculture	96.39	67.80
		Built-up	98.90	98.90
		River	95.59	96.30
		Urban open	96.77	95.24
		Urban green	66.12	97.56
		Waterbody	98.16	96.39
		Overall accuracy	91.92	
		Kappa coefficient	90.24	
2	Agra	Agriculture	91.60	82.76
		Built-up	100.00	98.23
		River	100.00	99.40
		Urban open	87.88	98.31
		Urban green	77.39	76.07
		Waterbody	100.00	98.75
		Forest	81.48	92.63
		Overall accuracy	91.63	
		Kappa coefficient	90.10	
3	Ahmedabad	Agriculture	84.75	90.91
		Built-up	93.75	91.84
		River	100.00	86.27
		Urban open	93.02	88.64
		Urban green	5.88	87.91
		Waterbody	71.01	100.00
		Overall accuracy	90.06	
		Kappa coefficient	0.88	
4	Allahabad	Agriculture	93.10	98.18
		Built-up	89.74	89.74
		River	79.17	79.17
		Urban open	97.50	97.50
		Urban green	94.44	89.47
		Waterbody	84.78	85.71
		Overall accuracy	107.09	
		Kappa coefficient	0.88	
5	Amritsar	Agriculture	72.31	85.45
		Built-up	98.13	98.13
		Urban open	97.40	87.21
		urban green	91.67	91.67
		Waterbody	100.00	97.30
		Overall accuracy	92.10	
		Kappa coefficient	0.90	
6	Asansol	Agriculture	88.96	78.38
		Built-up	100.00	97.94
		River	66.92	86.14
		Urban open	95.24	100.00
		Urban green	78.22	87.29
		Waterbody	100.00	84.24
		Overall accuracy	91.15	
		Kappa coefficient	0.89	
7	Aurangabad	Agriculture	91.73	89.05
		Built-up	89.38	100.00
		River	93.48	87.76
		Urban open	91.93	98.67
		Urban green	82.39	77.06
		Waterbody	95.29	98.78
		Forest	98.10	97.64
		Overall accuracy	91.81	
		Kappa coefficient	90.18	
8	Bangalore	Agriculture	85.42	82.00
		Built-up	83.33	62.50
		River	100.00	100.00
		Urban open	82.66	93.46
		urban green	81.63	83.33
		Waterbody	100.00	100.00
		Forest	93.88	95.83
		Overall accuracy	88.89	

S. No.	Cities	Accuracy (in percentage)		
		Classes	User	Producer
		Kappa coefficient	86.81	
9	Bhopal	Agriculture	91.11	91.11
		Built-up	83.33	61.22
		River	100.00	100.00
		Urban open	88.27	95.33
		Urban green	87.69	87.69
		Waterbody	100.00	100.00
		Forest	94.85	95.83
		Overall accuracy	92.66	
		Kappa coefficient	91.19	
10	Chandigarh	Agriculture	82.20	84.35
		Built-up	98.36	98.36
		River	100.00	91.57
		Urban open	94.35	99.40
		Urban green	72.88	66.15
		Waterbody	81.58	100.00
		Forest	91.49	86.00
		Overall accuracy	91.62	
		Kappa coefficient	89.99	
11	Chennai	Agriculture	82.95	84.88
		Built-up	92.00	94.52
		River	100.00	95.10
		Urban open	95.83	81.18
		Urban green	84.78	84.78
		Waterbody	89.25	91.21
		Bay	65.38	85.00
		Overall accuracy	88.40	
		Kappa coefficient	86.59	
12	Dehradun	Agriculture	90.45	90.96
		Built-up	98.06	96.19
		River	87.10	96.43
		Urban open	98.77	81.63
		Urban green	67.35	75.86
		Waterbody	100.00	100.00
		Forest	87.84	89.04
		Overall accuracy	89.01	
		Kappa coefficient	86.70	
13	Delhi (New Delhi)	Agriculture	76.36	87.50
		Built-up	95.00	93.44
		River	89.41	96.20
		Urban open	85.29	90.63
		Urban green	96.67	69.88
		Waterbody	74.07	95.24
		Forest	97.06	95.65
		Overall accuracy	88.84	
		Kappa coefficient	86.74	
14	Dhanbad	Agriculture	86.67	96.30
		Built-up	96.30	88.64
		River	100.00	98.46
		Urban open	96.59	77.98
		Urban green	89.36	84.85
		Waterbody	100.00	100.00
		Forest	98.11	92.86
		Mines	78.71	98.39
		Overall accuracy	91.09	
		Kappa coefficient	89.65	
15	Durg	Agriculture	90.97	78.77
		Built-up	97.67	98.82
		River	87.23	93.18
		Urban open	97.17	92.79
		Urban green	87.26	95.80
		Waterbody	97.84	95.77
		Overall accuracy	91.97	
		Kappa coefficient	89.70	
16	Faridabad	Agriculture	92.59	76.92
		Built-up	96.55	91.80
		River	96.00	98.36
		Urban open	90.91	85.71
		Urban green	73.33	86.84
		Waterbody	91.67	100.00
		Forest	81.16	98.25
		Overall accuracy	90.25	
		Kappa coefficient	88.61	
17	Gangtok	Agriculture	81.63	95.24
		Built-up	94.92	73.68
		River	94.12	98.46
		Urban open	98.88	90.72
		Urban green	88.89	77.42
		Waterbody	96.67	93.55
		Forest	92.50	90.24
		snow	73.33	91.67
		Overall accuracy	88.55	
		Kappa coefficient	86.86	
18	Ghaziabad	Agriculture	88.64	83.57
		Built-up	97.73	97.73
		River	79.31	88.46
		Urban open	97.56	93.75
		Urban green	84.80	91.77
		Waterbody	95.71	91.78
		Overall accuracy	91.03	
		Kappa coefficient	88.80	
19	Guwahati	Agriculture	97.14	87.18
		Built-up	95.74	97.83
		River	93.48	96.63
		Urban open	97.56	93.75
		Urban green	85.56	96.86

S. No.	Cities	Accuracy (in percentage)		
		Classes	User	Producer
		Waterbody	79.31	83.13
		Overall accuracy	91.75	
		Kappa coefficient	89.64	
20	Hyderabad	Agriculture	91.67	77.88
		Built-up	93.22	94.83
		River	94.52	80.23
		Urban open	90.74	97.03
		Urban green	70.73	84.06
		Waterbody	85.22	90.74
		Forest	85.96	89.09
		Overall accuracy	87.29	
		Kappa coefficient	85.02	
21	Indore	Agriculture	94.71	90.45
		Built-up	91.30	93.33
		River	86.54	93.75
		Urban open	96.00	92.31
		Urban green	84.16	88.54
		Waterbody	85.19	88.46
		Overall accuracy	91.54	
		Kappa coefficient	88.88	
22	Jabalpur	Agriculture	78.57	80.73
		Built-up	90.32	93.33
		River	100.00	88.89
		Urban open	92.47	99.26
		Urban green	92.73	89.08
		Waterbody	82.67	100.00
		Forest	94.37	90.54
		Overall accuracy	90.94	
		Kappa coefficient	89.12	
23	Jaipur	Agriculture	86.36	78.08
		Built-up	96.08	96.08
		River	91.67	81.48
		Urban open	88.06	92.19
		Urban green	84.11	84.91
		Waterbody	78.00	90.70
		Forest	89.74	92.11
		Overall accuracy	87.37	
		Kappa coefficient	86.91	
24	Jodhpur	Agriculture	86.67	85.53
		Built-up	100.00	97.37
		River	92.31	96.00
		Urban open	95.31	92.42
		Urban green	76.00	82.61
		Waterbody	94.83	90.16
		Overall accuracy	90.61	
		Kappa coefficient	80.15	
25	Kanpur	Agriculture	75.44	97.73
		Built-up	84.21	91.43

S. No.	Cities	Accuracy (in percentage)		
		Classes	User	Producer
		River	79.31	76.67
		Urban open	95.45	84.00
		Urban green	87.76	78.18
		Waterbody	95.83	92.00
		Overall accuracy	87.20	
		Kappa coefficient	84.39	
26	Kochi	Agriculture	75.76	72.46
		Built-up	94.74	98.36
		River	93.75	82.19
		Urban open	85.94	91.67
		Urban green	73.42	71.60
		Waterbody	81.94	93.65
		Bay	80.65	55.56
		Mangrove	89.61	94.52
		Overall accuracy	86.47	
		Kappa coefficient	83.91	
27	Kolkata	Agriculture	71.43	71.43
		Built-up	96.23	96.23
		Urban open	90.00	83.08
		Urban green	78.72	90.24
		Waterbody	100.00	97.96
		Overall accuracy	88.98	
		Kappa coefficient	0.86	
28	Kota	Agriculture	88.89	83.81
		Built-up	91.80	94.92
		River	97.78	91.67
		Urban open	89.61	94.52
		Urban green	82.76	88.89
		Waterbody	90.59	97.47
		Forest	87.50	80.00
		Overall accuracy	89.88	
		Kappa coefficient	88.14	
29	Lucknow	Agriculture	89.09	92.45
		Built-up	91.30	91.30
		Urban open	96.43	83.08
		Urban green	88.64	95.12
		Waterbody	100.00	95.24
		Overall accuracy	91.25	
		Kappa coefficient	0.88	
30	Ludhiana	Agriculture	83.61	86.44
		Built-up	96.15	96.15
		Urban open	95.83	80.70
		Urban green	87.95	96.05
		Waterbody	99.08	99.08
		Overall accuracy	92.92	
		Kappa coefficient	0.91	
31	Madurai	Agriculture	77.78	94.23
		Built-up	97.06	97.06

S. No.	Cities	Accuracy (in percentage)		
		Classes	User	Producer
		River	85.37	92.11
		Urban open	98.82	92.31
		Urban green	92.55	87.88
		Waterbody	96.39	93.02
		Overall accuracy	92.00	
		Kappa coefficient	90.14	
32	Mumbai	Agriculture	94.94	75.00
		Built-up	94.92	56.00
		River	100.00	100.00
		Urban open	98.78	82.00
		Urban green	96.80	133.00
		Waterbody	100.00	175.00
		Bay	73.56	64.00
		Mangrove	92.31	64.00
		Saltpan	71.52	136.00
		Overall accuracy	90.40	
		Kappa coefficient	0.89	
33	Mysore	Agriculture	86.15	82.35
		Built-up	94.87	98.67
		River	91.55	98.48
		Urban open	96.83	83.56
		Urban green	73.85	87.27
		Waterbody	98.21	90.16
		Overall accuracy	90.20	
		Kappa coefficient	88.23	
34	Nagpur	Agriculture	86.15	90.32
		Built-up	91.36	98.67
		River	91.55	98.48
		Urban open	96.00	77.42
		Urban green	80.00	84.21
		Waterbody	98.21	90.16
		Overall accuracy	90.34	
		Kappa coefficient	88.38	
35	Nashik	Agriculture	89.34	91.60
		Built-up	93.33	100.00
		River	93.62	96.70
		Urban open	97.03	85.22
		Urban green	77.59	84.91
		Waterbody	95.89	92.11
		Overall accuracy	91.82	
		Kappa coefficient	90.08	
36	Panaji	Agriculture	93.85	98.39
		Built-up	94.55	96.30
		River	100.00	71.54
		Urban open	95.70	98.89
		Urban green	97.76	95.62
		Waterbody	100.00	100.00
		Bay	70.27	97.50

S. No.	Cities	Accuracy (in percentage)		
		Classes	User	Producer
		Mangrove	96.74	94.68
		Saltpan	75.69	76.76
		Overall accuracy	90.83	
		Kappa coefficient	0.90	
37	Patna	Agriculture	81.16	83.58
		Built-up	97.10	97.10
		River	93.10	96.43
		Urban open	91.53	87.10
		Urban green	82.28	83.33
		Waterbody	95.95	92.21
		Overall accuracy	90.16	
		Kappa coefficient	88.16	
38	Pune	Agriculture	87.12	93.50
		Built-up	93.67	100.00
		River	100.00	91.84
		Urban open	92.68	88.37
		Urban green	86.79	100.00
		Waterbody	98.06	84.87
		Forest	100.00	84.87
		Overall accuracy	93.98	
		Kappa coefficient	0.93	
39	Rajkot	Agriculture	76.47	85.53
		Built-up	98.88	88.89
		River	94.23	97.03
		Urban open	94.55	81.25
		Urban green	80.61	89.77
		Waterbody	96.51	93.26
		Overall accuracy	89.94	
		Kappa coefficient	87.87	
40	Shimla	Agriculture	85.42	52.56
		Built-up	91.84	97.83
		River	93.55	100.00
		Urban open	96.70	93.62
		Forest	66.39	88.76
		Waterbody	100.00	94.23
		Overall accuracy	87.95	
		Kappa coefficient	85.39	
41	Srinagar	Agriculture	70.97	90.41
		Built-up	100.00	98.18
		River	90.63	100.00
		Urban open	96.25	92.77
		Forest	89.90	77.39
		Waterbody	100.00	90.32
		Overall accuracy	89.69	
		Kappa coefficient	87.49	
42	Surat	Agriculture	97.78	97.78
		Built-up	98.89	96.74
		River	100.00	84.42

S. No.	Cities	Accuracy (in percentage)		
		Classes	User	Producer
		Urban open	92.59	94.34
		Urban green	93.33	88.29
		Waterbody	97.09	100.00
		Bay	75.58	97.01
		Mangrove	87.76	94.51
		Saltpan	82.86	72.50
		Overall accuracy	91.85	
		Kappa coefficient	0.91	
43	Trichy	Agriculture	85.22	83.76
		Built-up	100.00	98.82
		River	90.32	87.50
		Urban open	96.08	90.74
		Urban green	87.72	92.59
		Waterbody	95.74	96.77
		Overall accuracy	92.24	
		Kappa coefficient	90.44	
44	Vadodara	Agriculture	86.41	79.46
		Built-up	94.92	98.25
		River	94.23	97.03
		Urban open	96.70	90.72
		Urban green	82.05	89.51
		Waterbody	98.45	96.94
		Overall accuracy	91.93	
		Kappa coefficient	90.04	
45	Varanasi	Agriculture	83.19	88.39
		Built-up	97.53	95.18
		River	92.00	95.83
		Urban open	96.74	81.65
		Urban green	86.21	92.59
		Waterbody	96.74	93.68
		Overall accuracy	90.84	
		Kappa coefficient	0.89	
46	Vasai-Virar	Agriculture	98.36	97.30
		Built-up	98.04	97.09
		River	100.00	88.00
		Urban open	95.12	83.87
		Urban green	97.06	79.52
		Waterbody	100.00	99.38
		Bay	50.86	94.68
		Mangrove	100.00	95.15
		Saltpan	90.91	78.43
		Overall accuracy	90.24	
		Kappa coefficient	0.89	
47	Vizag	Agriculture	93.94	97.48
		Built-up	93.75	93.75
		River	100.00	78.76
		Urban open	97.96	84.21
		Urban green	96.70	83.81
		Waterbody	100.00	100.00
		Bay	67.72	91.49
		Mangrove	100.00	96.91
		Saltpan	82.35	91.80
		Overall accuracy	91.43	
		Kappa coefficient	0.90	

References

Adejoke, A. O., & Badaru, Y. U. (2014). Accuracy assessment of pixel-based image classification of Kwali council area, Abuja, Nigeria. *Journal of Natural Science Research, 4*(22), 133–140.

Aguilar, C., Zinnert, J., Polo, M., & Young, D. (2012). NDVI as an indicator for changes in water availability to woody vegetation. *Ecological Indicators, 23,* 290–300.

Alrababah, M. A., & Alhamad, M. N. (2006). Land use/cover classification of arid and semi-arid Mediterranean landscapes using Landsat ETM. *International Journal of Remote Sensing*, *27*(13), 2703–2718. https://doi.org/10.1080/01431160500522700.

Amalisana, B., Rokhmatullah, & Hernina, R. (2017). Land cover analysis by using pixel-based and object-based image classification method in Bogor. In *The 5th geoinformation science symposium 2017 (GSS 2017): IOP conference series: Earth and environmental science* (p. 98).

Arevalo, V., González, J., Valdes, J., & Ambrosio, G. (2005). Detecting shadows in QuickBird satellite images. In *ISPRS Commission VII Mid-term symposium 'remote sensing: from pixels to processes'*. En-schede, The Netherland.

Arulbalaji, P., & Gurugnanam, B. (2014). Evaluating the normalized difference vegetation index using landsat data by ENVI in Salem district, Tamilnadu, India. *International Journal of Development Research, 4*(9), 1845–1846.

Atkinson, P., & Aplin, P. (2004). Spatial variation in land cover and choice of spatial resolution for remote sensing. *International Journal of Remote Sensing, 25*(18), 3687–3702. https://doi.org/10.1080/01431160310001654383.

Bartolucci, L., Robinson, B., & Silva, L. (1977). Field measurements of the spectral response of natural waters. *Photogrammetric Engineering and Remote Sensing, 43,* 595–598.

Bryant, N., Zobrist, A., Walker, R., & Gokhman, B. (1995). An analysis of Landsat thematic mapper P-product internal geometry and conformity to earth surface geometry. *Photogrammetric Engineering and Remote Sensing, 51,* 1435–1447.

Caetano, M. (Ed.). (2007). Image classification. Retrieved from ESA Advances Training Course on Land Remote Sensing.

Campbell, J., & Wynne, R. (2011). *Introduction to remote sensing*. New York: Guilford Press.

Chang, C.w., Shi, C., Liew, S. C., & Kwoh, L. (2014). Object-oriented land use cover classification of Landsat 8 OLI images in Sumatra. *International Geoscience and Remote Sensing Symposium (IGARSS)*. https://doi.org/10.1109/IGARSS.2014.6947422.

Chavez, P. (1989). Radiometric calibration of Landsat thematic mapper multispectral images. *Photogrammetric Engineering and Remote Sensing, 55,* 1285–1294.

Chavez, P. (1996). Image-based atmospheric corrections- revisited and improved. *Photogrammetric Engineering and Remote Sensing, 62*(9), 1025–1036.

Chen, Y., Dou, P., & Yang, X. (2017). Improving land use/cover classification with a multiple classifier system using AdaBoost integration technique. *Remote Sensing, 9*(10), 1055.

Choodarathnakara, A., Kumar, A., Koliwad, S., & Patil, G. (2012). Mixed pixels: A challenge in remote sensing data classification for improving performance. *International Journal of Advanced Research in Computer Engineering & Technology (IJARCET), 1*(9), 261.

Congalton, R., & Green, K. (2019). *Assessing the accuracy of remotely sensed data: Principles and practices* (3rd ed.). Boca Raton: CRC Press.

Coppin, P., Jonckheere, I., Nackaerts, K., Muys, B., & Lambin, E. (2004). Digital change detection methods in ecosystem monitoring: A review. *International Journal of Remote Sensing, 25*(9), 1565–1596.

DeFries, R., & Chan, J.-W. (2000). Multiple criteria for evaluating machine learning algorithms for land cover classification from satellite data. *Remote Sensing of Environment, 74*(3), 503–515. https://doi.org/10.1016/S0034-4257(00)00142-5.

Demir, B., Minello, L., & Bruzzone, L. (2014). Definition of effective training sets for supervised classification of remote sensing images by a novel cost-sensitive active learning method. *IEEE Transactions on Geoscience and Remote Sensing, 52*(2), 1272–1284.

Di Gregorio, A., & Jansen, L. (1998). A new concept for a land-cover classification system. *Land, 2*(1), 55–65.

Dorren, L., Maier, B., & Seijmonsbergen, A. (2003). Improved Landsat-based forest mapping in steep mountainous terrain using object-based classification. *Forest Ecology and Management, 183*(1–3), 31–46.

Dronova, I. (2015). Object-based image analysis in wetland research: A review. *Remote Sensing, 7*(5), 6380–6413.

Duong, N. (2012). Waterbody extraction from multispectral image by spectral pattern analysis. In *International archives of the photogrammetry, remote sensing and spatial information sciences* (pp. 181–186). Melbourne: XXII ISPRS Congress.

Fichera, C., Modica, G., & Pollino, M. (2012). Land Cover classification and change-detection analysis using multi-temporal remote sensed imagery and landscape metrics. *European Journal of Remote Sensing, 45*(1), 1–18.

Friedl, M., & Brodley, C. (1997). Decision tree classification of land cover from remotely sensed data. *Remote Sensing of Environment, 61*(3), 399–409.

Garg, A., Avashia, V., & Parihar, S. (2018). *Land use change trends of Indian cities: A bird's-eye view-vulnerabilities of unplanned urban growth*. New Delhi: Sage India.

Green, E., Mumby, P., Edwards, A., & Clark, C. (1996). A review of remote sensing for the assessment and management of tropical coastal resources. *Coastal Management, 24*(1), 1–40.

Guha, S. (2016). Capability of NDVI technique in detecting mangrove vegetation. *International Journal of Advanced Biological Research, 6*(2), 253–258.

Hecher, J., Filippi, A., Guneralp, I., & Paulus, G. (2012). Extracting River features from remotely sensed data: An evaluation of thematic correctness (Doctoral dissertation, Department of Geography, Texas A&M University), pp. 187–196.

Holben, B. (1986). Characteristics of maximum-value composite images from temporal AVHRR data. *International Journal of Remote Sensing, 7*(11), 1417–1434.

Hua, L., Man, W., Wang, Q., & Zhao, X. (2012). A new decision tree classification approach for extracting urban land from Landsat TM in a coastal city, China. In *Fourth international symposium on information science and engineering*, (pp. 282–286).

Hussain, M., Chen, D., Cheng, A., Wei, H., & Stanley, D. (2013). Change detection from remotely sensed images: From pixel-based to object-based approaches. *ISPRS Journal of Photogrammetry and Remote Sensing, 80,* 91–106.

Islam, K., Jashimuddin, M., Nath, B., & Nath, T. K. (2018). Land use classification and change detection by using multi-temporal remotely sensed imagery: the case of Chunati wildlife sanctuary, Bangladesh. *The Egyptian Journal of Remote Sensing and Space Science*, *21*(1), 37–47. https://doi.org/10.1016/j.ejrs.2016.12.005.

Kantakumar, L., & Neelamsetti, P. (2015). Multi-temporal land use classification using hybrid approach. *The Egyptian Journal of Remote Sensing and Space Science, 18*(2), 289–295.

Keuchel, J., Naumann, S., Heiler, M., & Siegmund, A. (2003). Automatic land cover analysis for Tenerife by supervised classification using remotely sensed data. *Remote Sensing of Environment, 86*(4), 530–541. https://doi.org/10.1016/S0034-4257(03)00130-5.

Kindu, M., Schneider, T., Teketay, D., & Knoke, T. (2013). Land use/land cover change analysis using object-based classification approach in Munessa-Shashemene landscape of the Ethiopian highlands. *Remote Sensing, 5*(5), 2411–2435.

Klein-Gebbinck, M. S. (1998). *Decomposition of mixed pixels in remote sensing images to improve the area estimation of agricultural fields*. Veenendaal: University of Nijmegen, University Press.

Lee, L., Chen, L., Wang, X., & Zhao, J. (2011). Use of Landsat TM/ETM+ data to analyze urban heat island and its relationship with land use/cover change. In *International conference on remote sensing, environment and transportation engineering* (pp. 922–927).

Li, M., Zang, S., Zhang, B., Li, S., & Wu, C. (2014). A review of remote sensing image classification techniques: The role of spatio-contextual information. *European Journal of Remote Sensing, 47*(1), 389–411.

Lioy, P., & Kneip, T. (1980). Aerosols: Anthropogenic and natural sources and transport. *Journal of Air Pollution Control Association, 30*(4), 358–361.

Liu, W., Gopal, S., & Woodcock, C. (2004). Uncertainty and confidence in land cover classification using a hybrid classifier approach. *Photogrammetric Engineering and Remote Sensing, 70*(8), 963–971.

Liu, J., & Mason, P. (2009). *Essential image processing and GIS for remote sensing*. Hoboken: Wiley.

Lu, D., & Weng, Q. (2007). A survey of image classification methods and techniques for improving classification performance. *International Journal of Remote Sensing, 28*(5), 823–870.

Luus, F., Salmon, B., van den Bergh, F., & Maharaj, B. (2015). Multiview deep learning for land-use classification. *IEEE Geoscience and Remote Sensing Letters, 12*(12), 2448–2452.

Ma, L., Li, M., Ma, X., Cheng, L., Du, P., & Liu, Y. (2017). A review of supervised object-based land-cover image classification. *ISPRS Journal of Photogrammetry and Remote Sensing, 130,* 277–293. https://doi.org/10.1016/j.isprsjprs.2017.06.001.

Mandal, J., Ghosh, N., & Mukhopadhyay, A. (2019). Urban growth dynamics and changing land-use land-cover of megacity Kolkata and its environs. *Journal of the Indian Society of Remote Sensing, 47,* 1707–1725. https://doi.org/10.1007/s12524-019-01020-7.

Manandhar, R., Odeh, I., & Ancev, T. (2009). Improving the accuracy of land use and land cover classification of landsat data using post-classification enhancement. *Remote Sensing.*, *1*(3), 330–344. https://doi.org/10.3390/rs1030330.

Masocha, M., & Skidmore, A. (2011). Integrating conventional classifiers with a GIS expert system to increase the accuracy of invasive species mapping. *International Journal of Applied Earth Observation and Geoinformation (JAG), 13*(3), 487–494.

Mather, P., & Koch, M. (2011). *Computer processing of remotely-sensed images: An introduction* (4th ed.). Hoboken: Wiley.

Mather, P., & Tso, B. (2009). *Classification methods for remotely sensed data* (2nd ed.). Boca Raton: CRC Press.

McCallum, I., Obersteiner, M., Nilsson, S., & Shvidenko, A. (2006). A spatial comparison of four satellite derived 1 km global land cover datasets. *International Journal of Applied Earth Observation and Geoinformation, 8*(4), 246–255.

Meer, M., & Mishra, A. (2020). Remote sensing application for exploring changes in land-use and land-cover over a district in Northern India. *Journal of the Indian Society of Remote Sensing*. https://doi.org/10.1007/s12524-019-01095-2.

Meyer, W., & Turner, B., II. (1992). Human population growth and global land-use/cover change. *Annual Review of Ecology and Systematics, 23,* 39–61.

Mohammady, M., Moradi, H., Zeinivand, H., & Temme, A. (2015). A comparison of supervised, unsupervised and synthetic land use classification methods in the north of Iran. *International Journal of Environmental Science and Technology, 12,* 1515–1526.

Morfitt, R., Storey, J., Choate, M., Rengarajan, R., & Lubke, M. (2017). *Landsat 8 geometry status*. Sioux Falls: USGS Earth Resources Observation and Science (EROS) Center.

Moskal, L. M., Styers, D. M., & Halabisky, M. (2011). Monitoring urban tree cover using object-based image analysis and public domain remotely sensed data. *Remote Sensing, 3*(10), 2243–2262.

Nazmfar, H., & Jafarzadeh, J. (2018). Classification of satellite images in assessing urban land use change using scale optimization in object-oriented processes (A case study: Ardabil city, Iran). *Journal of the Indian Society of Remote Sensing, 46,* 1983–1990. https://doi.org/10.1007/s12524-018-0850-7.

Nicholas, C. T. (2012). *Land use/land cover classification: Methods to overcome pixel confusion and the effects of tree shadows in very high resolution multispectral imagery*. Maryville: Northwest Missouri State University.

Pal, M., & Mather, P. (2003). An assessment of the effectiveness of decision tree methods for land cover classification. *Remote Sensing of Environment, 86*(4), 554–565. https://doi.org/10.1016/S0034-4257(03)00132-9.

Parthasarathy, R., Baranwal, A., Gupta, M., & Parihar, S. (2014). P5 shoreline changes in south Gujarat coast: Understanding linkages, threats and impacts.

Peña, J., Gutiérrez, P., Hervás-Martínez, C., Six, J., Plant, R., & López-Granados, F. (2014). Object-based image classification of summer crops with machine learning methods. *Remote Sensing, 6*(6), 5019–5041.

Phiri, D., & Morgenroth, J. (2017). Developments in landsat land cover classification methods: A review. *Remote Sensing, 9*(9), 967.

Rahman, M.d., Ullah, R., & Lan, M., Sri Sumantyo, J., Kuze, H., & Tateishi, R. (2013). Comparison of Landsat image classification methods for detecting mangrove forests in Sundarbans. *International Journal of Remote Sensing, 34*, 1041–1056. https://doi.org/10.1080/01431161.2012.717181.

Ramachandran, R., & Reddy, C. (2017). Monitoring of deforestation and land use changes (1925–2012) in Idukki district, Kerala, India using remote sensing and GIS. *Journal of the Indian Society of Remote Sensing, 45,* 163–170. https://doi.org/10.1007/s12524-015-0521-x.

Rozenstein, O., & Karnieli, A. (2011). Comparison of methods for land-use classification incorporating remote sensing and GIS inputs. *Applied Geography, 31*(2), 533–544.

Rwanga, S., & Ndambuki, J. (2017). Accuracy assessment of land use/land cover classification using remote sensing and GIS. *International Journal of Geosciences.*, *8*, 611–622. https://doi.org/10.4236/ijg.2017.84033.

Sader, S. A., Ahl, D., & Liou, W. S. (1995). Accuracy of Landsat-TM and GIS rule-based methods for forest wetland classification in Maine. *RemoteSensing of Environment*, *53*, 133–144.

Schowengerdt, R. (2006). *Remote sensing: Models and methods for image processing*. Cambrigde: Academic Press.

Schweitzer, C., Rücker, G., Conrad, C., Strunz, G., & Bendix, J. (2005). *'Knowledge-based land use classification combining expert knowledge, GIS, multi-temporal Landsat 7 ETM+ and MODIS time series data in Khorezm*. Uzbekistan: Göttingen GIS & Remote Sensing Days.

Shahtahmassebi, A., Yang, N., Wang, K., Moore, N., & Shen, Z. (2013). Review of shadow detection and de-shadowing methods in remote sensing. *Chinese Geographical Science, 23,* 403–420.

Sharma, R., Ghosh, A., & Joshi, P. (2013). Decision tree approach for classification of remotely sensed satellite data using open source support. *Journal of Earth System Science, 122,* 1237–1247.

Sharma, K., Jain, S., & Garg, P. (1984). Monitoring landuse and landcover changes using landsat images. *Journal of the Indian Society of Photo-Interpretation and Remote Sensing, 12,* 65–70.

Son, N., Chen, C., Chang, N., Chen, C., Chang, L., & Thanh, B. (2015). Mangrove mapping and change detection in Ca Mau Peninsula, Vietnam, using landsat data and object-based image analysis. *IEEE Journal of Selected Topics in Applied Earth Observations and Remote Sensing, 8*(2), 503–510. https://doi.org/10.1109/JSTARS.2014.2360691.

Song, X.-P., Huang, C., Feng, M., Sexton, J., Channan, S., & Townshend, J. (2014). Integrating global land cover products for improved forest cover characterization: An application in North America. *International Journal of Digital Earth, 7*(9), 709–724.

Steele, B. (2000). Combining multiple classifiers: An application using spatial and remotely sensed information for land cover type mapping. *Remote Sensing of Environment, 74*(3), 545–556. https://doi.org/10.1016/S0034-4257(00)00145-0.

Storey, J., & Choate, M. (2000). Landsat 7 on-orbit geometric calibration and performance. In *Proceedings of SPIE-The international society for optical engineering*.

Tampubolon, T., Abdullah, K., & Hwee, L. (2013). Comparison of pixel and object based approaches using landsat data for land use and land cover classification in coastal zone of Medan, Sumatera. *International Journal of Tomography & Simulation, 24*(3).

Tarantino, E., Novelli, A., Aquilino, M., Figorito, B., & Fratino, U. (2015). Comparing the MLC and JavaNNS approaches in classifying multi-temporal LANDSAT satellite imagery over an ephemeral river area. *International Journal of Agricultural and Environmental Information Systems (IJAEIS), 6*(4), 20.

Tewolde, M., & Cabral, P. (2011). Urban sprawl analysis and modeling in Asmara, Eritrea. *Remote Sensing, 3,* 2148–2165.

Tilahun, A., & Teferie, B. (2015). Accuracy assessment of land use land cover classification using google earth. *American Journal of Environmental Protection*, *4*, 193–198. https://doi.org/10.11648/j.ajep.20150404.14.

Tucker, C., Grant, D., & Dykstra, J. (2004). NASA's global orthorectified Landsat data set. *American Society for Photogrammetry and Remote Sensing, 10*(3), 313–322.

Vaz, E., Taubenböck, H., Kotha, M., & Arsanjani, J. (2017). Urban change in Goa, India. *Habitat International, 68,* 24–29.

Wang, X., & Chen, X. (2012). Classification of ASTER image using SVM and local spatial statistics Gi. In *International conference on computer vision in remote sensing*, (pp. 366–370). Xiamen.

Warrender, C., & Augusteijn, M. (1999). Fusion of image classifications using Bayesian techniques with Markov random fields. *International Journal of Remote Sensing, 20*(10), 1987–2002.

Wulder, M., Masek, J., Cohen, W., Loveland, T., & Woodcock, C. (2012). Opening the archive: How free data has enabled the science and monitoring promise of Landsat. *Remote Sensing of Environment, 122,* 2–10.

Yang, C.-C., Prasher, S., Enright, P., Madramootoo, C., Burgess, M., Goel, P., et al. (2003). Application of decision tree technology for image classification using remote sensing data. *Agricultural Systems, 76,* 1101–1117.

Zhan, Q. (2003). *A hierarchical object- based approach for urban land-use classification from remote sensing data*. Enschede: International Institute for Geo-Information Science and Earth Observation.

Zhang, Q., Wang, J., Peng, X., Gong, P., & Shi, P. (2002). Urban built-up land change detection with road density and spectral information from multi-temporal Landsat TM data. *International Journal of Remote Sensing, 23*(15), 3057–3078. https://doi.org/10.1080/01431160110104728.

Zhao, P., Zhao, J., Wu, J., Yang, Y., Xue, W., & Hou, Y. (2016). Integration of multi-classifiers in object-based methods for forest classification in the Loess plateau, China. *ScienceAsia, 42,* 283–289.